Operator & fractional order-based robust nonlinear control for the spiral heat exchanger

September, 2022

Guanqiang Dong

The Graduate School of Engineering
(Doctor's Course)
TOKYO UNIVERSITY OF
AGRICULTURE AND TECHNOLOGY

Acknowledgements

I am over helmed in all humbleness and gratefulness to acknowledge my depth to all those who have helped me. Their immense knowledge and plentiful experience have encouraged me in all the time of my academic research and daily life.

First, I would like to express my sincere gratitude to express my sincere thanks to my supervisor, Professor Mingcong Deng, for their invaluable advice, continuous support, and patience during my PhD study. Their immense knowledge and plentiful experience have encouraged me in all the time of my academic research and daily life.

Second, I want to show my real gratitude to a brilliant array of professors in the university. All of them have deepened my admiration for science, I want especially, to thank Professor Yasuhiro Takaki, Kenta Umebayashi, Takuji Arima, Ya Zhang, for their brilliant comments on my dissertation, which have greatly enabled me to improve the dissertation for better. Next, I am indebted to Dr. Xudong Gao, Dr. Yanfeng Wu, Dr. Guang Jin, Mrs. Ximei Li, Mrs. Yuanhong Xu, Mrs. Izumi Fukukawa, and other members of Deng laboratory for their advices and kind help. We have worked together, suffered the frustration of our work together and shared the joy of our every little success together.

Finally, I would like to express my gratitude to my parents, my wife and my children. Without their tremendous understanding and encouragement in the past few years, it would be impossible for me to complete my study.

Summary

This dissertation provides operator & fractional order-based nonlinear robust control for the spiral heat exchanger with uncertainties and disturbances described by the fractional order model. Under disturbances, the aim of this dissertation is to guarantee the robust stability, tracking performance and anti-disturbance ability of the spiral heat exchanger with uncertainties.

Heat exchangers are commonly used in various industries. A spiral heat exchanger is a compact plant that only requires a small space for installation compared to traditional heat exchanger solutions and is excellent in high heat transfer efficiency. However, the spiral heat exchanger is a nonlinear plant with uncertainties and it needs to consider the difference between the heat medium, the heated medium and the other factors. In some applications, the output temperature of heated or cooled fluid for the heat exchanger must be controlled accurately. Because the heat transfer coefficient is impacted by various factors such as fluid flow, condition pressure, the uncertainties, the error of the mathematical model, and a long-time delay, etc., it is difficult to accurately model and control the output temperature of the heat exchanger.

Firstly, a parallel fractional order derivative model is proposed by considering the merit of the graphics processing unit (GPU) in this dissertation. A parallel fractional order derivative model for the spiral heat exchanger is constructed. Simulations show the relationships between the output temperature of heated fluid and the orders of fractional order derivatives with two directional fluids impacted by complex factors, namely, the volume flow rate in hot fluid, and the volume flow rate in cold fluid, respectively.

Secondly, this dissertation studies operator & fractional order based nonlinear robust control for the spiral counter-flow heat exchanger with uncertainties under disturbances. Operator fractional order controller and fractional order PID (FOPID) controller are designed and some parameters are tuned by

trial-and-error method. Simulations verify tracking and anti-disturbance performance by comparison of different control cases.

Finally, operator based nonlinear fractional order robust control for the spiral heat exchanger described by a parallel fractional order model is proposed. The parallel fractional order model for the spiral heat exchanger is identified by particle swarm Optimization (PSO). FOPID controller and operator controller for the spiral heat exchanger are designed under parallel fractional order mathematical model. The parameters of FOPID controller are optimized by PSO. Comparisons of two control cases are performed, and the effectiveness is illustrated.

Contents

List of Figures

List of Tables

Chapter 1

Introduction

1.1 Background

A heat exchanger is the most used in the industry such as space heating, refrigeration, air conditioning, power stations, chemical plants, petrochemical plants, petroleum refineries, natural-gas processing, and sewage treatment. It uses the principle of heat transfer between two or more fluids to transfer the heat energy of the high temperature heat fluid to the low temperature heat fluid in order to heating the low temperature fluid or cooling the high temperature heat fluid, which has the idea of energy saving [1–5]. A spiral-plate heat exchanger is a compact plant that only requires a small space for installation compared to traditional heat exchanger solutions and has excellent in high heat transfer efficiency (See [6–9]). However, the spiral-plate heat exchanger is a nonlinear plant with uncertainties thinking of the difference between the heat medium, the heated medium and the other factors. In some applications, the output temperature heated or cooled for the heat exchanger must be controlled accurately. Because the heat transfer coefficient of the heat exchanger is impacted by various factors such as fluid flow, condition pressure, the uncertainties, the error of the mathematical model, and a long-time delay, etc., so it is difficult to be accurately modelled and controlled. In the past

few years, the research of heat exchangers has mainly focused on the design of heat exchangers [10–12]. In some papers (Such as [13, 14]), an effective internal fluid mathematical model is established by using the heat balance law between the two fluids. Only the effect of the flow velocity on the heat transfer coefficient, but not the effect of the two fluid flows velocity on the heat transfer time is considered.

Fractional order derivatives as an extension of integer order derivatives have been widely used to describe practical application objects following their first being proposed by Leibniz in 1695 [15]. The research of the theory and applications to fractional order calculus and derivative (Such as in solution of fractional order calculus and derivative [16–22] and stability [23–30]) expanded greatly over the 20th and 21st centuries. Now, fractional order calculus and derivative were used in various fields such as engineering, physics, chemistry, and hydrology etc. in recent years. Although the use of integer order derivatives to describe dynamic systems applications using traditional methods has a clear physical geometric interpretation, in certain real-world applications dynamic systems described by fractional order derivatives can be more accurate than those described by integer order derivatives; examples include viscoelastic systems, liquids, heat diffusion and dielectric polarization, electrode-electrolyte polarization, nonlinear thermoelastic system etc. [31–38]. Thus, a heat exchanger is suitable for description by fractional order derivative [39–46]. In a feedback control system, a proportion integral derivative (PID) control with only three parameters to tune is widely used thanks to its simple structure and high robustness. For nonlinear control systems with large delay times and disturbances, it is difficult to achieve good control performance. Fractional order PID (FOPID) control extends the conventional PID controller, having five parameters to tune and being more flexible than the traditional PID controller. FOPID control has better control performance in applications, as proven by many studies in recent years [47–60]. Fractional

order controllers were being used extensively by many researchers to achieve the better robust performance in both the linear and the nonlinear systems. In [32], nonlinear thermoelastic fractional-order model of nonlocal plates is studied. Reference [33] proposed a fractional nonlocal elasticity model. They show elasticity model described by fractional order derivative is more accurate than the traditional system described by integer order in theory and application [61]. In control systems, modeling, stability, controllability, observability is very important for performance. In fractional order system, these need to be considered in [34, 36, 61, 62], too. Nowadays, fractional order calculus and derivative are still the absence of solution method and rapid computing algorithm [63].

GPU (That is graphics processing unit), which provides more computing units and high data bandwidth in a limited area [64]. It is originally developed for graphics applications, now, it has been increasingly applied to do parallel computing in scientific and engineering. GPU has higher execution efficiency for parallel data, and the more data parallelism, the higher the execution efficiency. CUDA is a software and hardware system that can make GPU work as a device for data parallel computing [65, 66].

Nonlinear robust control is a problem that has been considered by many researchers in many different fields. In [13], the authors consider the right coprime factorization needed to compensate for the nonlinearity of the system and provide robust control performance in an improved system. The right coprime factorization suit is required for both linear feedback control and nonlinear feedback control. This provides a convenient approach to study the input–output stability of nonlinear feedback control systems. In [39–41,67], the authors studied robustness using right coprime factorization of a nonlinear system with perturbations. Operator-based nonlinear robust control is a simple method to improve stability and anti-disturbance using only the output signal of the plant.

A spiral heat exchanger is a nonlinear system with several uncertainties and many disturbances in the changes in the flow rate, fluid temperature, fluid density, fluid pressure on the two fluids side, etc., as well as a large delay time. It is very difficult to control under complex operating conditions. In application, the spiral heat exchanger mathematical model described via fractional order differential equation is more accurate than other methods [37, 61, 68, 69]. Therefore, motivated by the above references, this paper presents a mathematical model of a spiral heat exchanger using a fractional order derivative system. Operator-based fractional order control is employed to improve robustness in a nonlinear system with uncertainties, disturbances, and a high delay time. A fractional order operator controller and fractional order PID controller are designed to account for uncertainties and disturbance, and the different control cases in tracking performance and stability are analyzed. Finally, the proposed control schemes are simulated and analyzed. This dissertation focuses on verifying operator and fractional order nonlinear robust control for a spiral counter-flow heat exchanger with uncertainties and disturbances by simulatio. In the future, we intend to study operator and fractional order nonlinear robust control for a spiral counter-flow heat exchanger with uncertainties and disturbances using experimental equipment to determine the optimal parameters for fractional order PID control, and to study MIMO control problems using fractional order derivatives [71-89]

1.2 Fractional order PID control

The differential equation of fractional order controller $PI^{\lambda}D^{\delta}$ [55–58]is described by

$$u(t) = K_{p1}e(t) + K_i D_t^{-\lambda} e(t) + K_d D_t^{\delta} e(t) \tag{1.1}$$

If $\lambda, \delta = 1$, it is a conventional PID control. It is obvious that the fractional order controller needs to design the three parameters K_{p1}, K_i, and K_d as well

as the orders λ, δ of the integral and derivative controllers. The orders λ, δ need not necessarily be integers, and can be any real numbers. As shown in Figure 4.1, the FOPID (fractional order PID) controller generalizes the conventional integer order PID controller and expands it from point to plane. This expansion can provide a great deal more flexibility in PID control design.

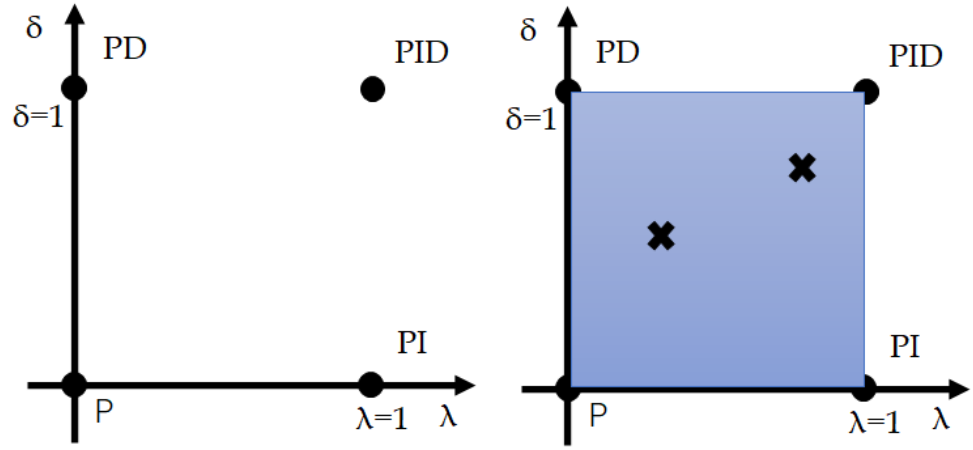

Figure 1.1: FOPID controller

1.3 Motivation

In this dissertation, a spiral heat exchanger described by a parallel fractional order model with uncertainties and disturbances is conducted. Operator & fractional order based noninear robust contol for the spiral heat exchanger is proposed and paramters of fractional order PID are optimized by MPSO for improving control performnce.

First, references [32, 33, 61] show elasticity model described by fractional order derivative is more accurate than the traditional system described by integer order in theory and application [17]. Fractional order derivative equation is more suitable to describe thermoelastic model than integer order equation.

Heat transfer for the heat exchanger is thermoelastic model. Therefore, it is motivated by the above references. Traditionally, a spiral-plate heat exchanger mathematical model is constructed by integer order derivative equation. A spiral-plate heat exchanger mathematical model constructed by fractional order derivative equation is more accurate than conventional method. So, a parallel fractional order derivative model is proposed by considering the merits of GPU and fractional order derivative. Further, parallel fractional order derivation model for the spiral heat exchanger is constructed. The parallel fractional order derivation model for the spiral-plate heat exchanger executes faster than traditional model and can quickly reply to disturbance. In the future, we will study operator-based robust nolinear control system for the spiral heat exchanger by using the proposed parallel model [39–41].

A spiral heat exchanger is a nonlinear system with several uncertainties and many disturbances in the changes in the flow rate, fluid temperature, fluid density, fluid pressure on the two fluids side, etc., as well as a large delay time. It is very difficult to control under complex operating conditions. In application, the spiral heat exchanger mathematical model described via fractional order differential equation is more accurate than other methods [37, 61, 68, 69]. Therefore, motivated by the above references, this paper presents a mathematical model of a spiral heat exchanger using a fractional order derivative system. Operator-based fractional order control is employed to improve robustness in a nonlinear system with uncertainties, disturbances, and a high delay time. A fractional order operator controller and fractional order PID controller are designed to account for uncertainties and disturbance, and the different control cases in tracking performance and stability are analyzed. Finally, the proposed control schemes are simulated and analyzed. This disseration focuses on verifying operator and fractional order nonlinear robust control for a spiral counter-flow heat exchanger with uncertainties and disturbances by simulation. In summary, the disseration proposed operator

& fractional order based nonlinear rubust control for a spiral heat exchanger.

1.4 Contribution

In this disseration operator & fractional order based nonlinear robust control for the spiral heat exchanger described by fractional order model is proposed. Three main contributions are as follows. First,a parallel fractional order derivative model is proposed by considering the merits of GPU and fractional order derivative. Further, parallel fractional order derivation model for the spiral heat exchanger is constructed. The parallel fractional order derivation model for the spiral-plate heat exchanger executes faster than traditional model and can quickly reply to disturbance.

Second, the disseration proposed operator & fractional order based nonlinear robust control for the spiral heat exchanger. Operator-based fractional order nonlinear robust control is employed to improve robustness in a nonlinear system with uncertainties, disturbances. A fractional order operator controller and fractional order PID controller are designed to account for uncertainties and disturbances, and the different control cases in tracking performance and stability are analyzed. Finally, the proposed control schemes are simulated and analyzed. This disseration focuses on verifying operator and fractional order nonlinear robust control for the spiral counter-flow heat exchanger with uncertainties and disturbances by simulation.

Third, operator based nonlinear fractional order robust control for the spiral heat exchanger described by parallel fractional order model is proposed. The parallel fractional order model for the spiral heat exchanger is identified by PSO. Fractional order PID controller and operator controller for the spiral heat exchanger are design under identified parallel fractional order mathematical model. The parameters of FOPID controller are optimized by PSO. Finally, comparisons of two control cases are performed, and the

effectiveness is illustrated.

1.5 Organization

The organization of the rest dissertation can be summarized as follows:

In Chapter 2, the fractional order preliminaries and operator theoretical background to remaining the following chapters of this dissertation is given. It also presents a spiral heat exchanger.

In Chapter 3, a parallel fractional order derivation model is proposed by considering the merit of the graphics processing unit (GPU). Then, the parallel fractional order derivation model for the spiral-plate heat exchanger is constructed. Simulations show the relationships between the output temperature of heated fluid and the orders of fractional order derivatives with two directional fluids impacted by complex factors, namely, the volume flow rate in hot fluid, and the volume flow rate in cold fluid, respectively.

Chapter 4 studies operator & fractional order based nonlinear robust control for the spiral counter-flow heat exchanger with uncertainties under disturbances. Operator fractional order controller and fractional order PID (FOPID) controller are designed and some parameters are tuned by trial-and-error method. Simulations verify tracking and anti-disturbance performance by comparison of different control cases.

In chapter 5, operator based nonlinear fractional order robust control for the spiral heat exchanger described by a parallel fractional order model is proposed. The parallel fractional order model for the spiral heat exchanger is identified by PSO. Fractional order PID controller and operator controller for the spiral heat exchanger are design under parallel fractional order mathematical model. The parameters of FOPID controller are optimized by PSO. Finally, comparisons of two control cases are performed, and the effectiveness is illustrated.

In Chapter 6, the proposed operator & frctional order based robust nonlinear control for the spiral heat exchanger is summarized. Simulations and/or experiments have confirm their effectiveness.

Chapter 2

Mathematical preliminaries and problem statement

2.1 Introduction

In this chapter, the fractioal order preliminaries and operator theoretical background to remaining the following chapters of this dissertation is given. It also presents a spiral heat exchanger.

In Section 2.2, the definitions fractional order derivative and integeral are introduced.

In Section 2.3, operator and frctional order based rubust nonlinear control method is presented.

In Section 2.4, Particle swarm optimization is introduced.

In Section 2.5, the problem discussed in this dissertation is presented.

In Section 2.6, the conclusion of this chapter is given.

2.2 Fractional order derivative and integeral

A basic overview of fractional order integral and operator theory are presented in this section.

Definition 2.2.1 (The definition of Caputo's fractional order calculus [15])**.**

$$D^{-\beta}f(t) = \frac{1}{\Gamma(\beta)}\int_a^t (t-\tau)^{\beta-1}f(\tau)d(\tau), \beta > 0 \tag{2.1}$$

where $\Gamma(\cdot)$ is Gamma function, $\Gamma(\epsilon) = \int_0^\infty e^{-t}t^{\epsilon-1}$.

Definition 2.2.2 (The definition of Caputo's fractional order derivative [15])**.**

$${}_a^C D_t^q f(t) = \frac{1}{\Gamma(n-q)}\int_a^t \frac{f^{(n)}(t)}{(t-\tau)^{n-q-1}}d\tau, n-1 < q < n \tag{2.2}$$

where n is a integer that is equal to or greater than q. If n = 1, then $0 < q < 1$.

$${}_a^C D_t^q f(t) = \frac{1}{\Gamma(1-q)}\int_a^t \frac{f'(t)}{(t-\tau)^{-q}}d\tau \tag{2.3}$$

2.3 Operator & fractional order-based robust nonlinear control approach

2.3.1 Lipschitz Operators

Definition 2.3.1 ([72])**.** Let X^e and Y^e be two extended linear spaces which are associated, respectively, with two Banch spaces, X and Y, of measurable functions defined on the time domain $[0, \infty)$, and let D be a subset of X^e. A nonlinear operator $A : D \to Y^e$ is called a generalized Lipschitz operator on D if there exists a constant L such that

$$\|[A(x)]_T - [A(\tilde{x})]_T\|_Y \leq L\|x_T - \tilde{x}_T\|_X$$

for all $x, \tilde{x} \in D$ and for all $T \in [0, \infty)$.
Note that the least such constant L is provided by

$$\|A\| := \sup_{T\in[0,\infty)} \sup_{\substack{x,\tilde{x}\in D \\ x_T \neq \tilde{x}_T}} \frac{\|[A(x)]_T - [A(\tilde{x})]_T\|_Y}{\|x_T - \tilde{x}_T\|_X} \tag{2.4}$$

which is a semi-norm for general nonlinear operators and is the actual norm for linear operator A. The actual norm for a nonlinear operator A is provided by

$$\begin{aligned}\|A\|_{Lip} &= \|A(x_0)\|_Y + \|A\| \\ &= \|A(x_0)\|_Y + \sup_{T\in[0,\infty)} \sup_{\substack{x,\tilde{x}\in D \\ x_T\neq\tilde{x}_T}} \frac{\|[A(x)]_T - [A(\tilde{x})]_T\|_Y}{\|x_T - \tilde{x}_T\|_X}\end{aligned} \tag{2.5}$$

for any fixed $x_0 \in D$.

Theorem 1. *Let X^e and Y^e be two extended linear spaces which are associated, respectively, with two Banch spaces, X and Y, of measurable functions defined on the time domain $[0,\infty)$, and let D be a subset of X^e. A nonlinear operator A_d fractional order operation, defined in [72], is a generalized Lipschitz operator on D.*

Proof. Let $A_d(x)$, meaning mapping from $x \to A_d$, where A_d is a fractional order operation. For any $x_1, x_2 \in X^e$; however, $x_1 \neq x_2$ extended linear space.

$$\begin{aligned}\|A_d(x_1) - A_d(x_2)\| &= \|D_x^q(x_1) - D_x^q(x_2)\| \\ &= \|\frac{1}{\Gamma(n-q)}\int_a^t \frac{x_1^{(n)}(\tau)}{(t-\tau)^{n-q-1}}d\tau - \frac{1}{\Gamma(n-q)}\int_a^t \frac{x_2^{(n)}(\tau)}{(t-\tau)^{n-q-1}}d\tau\|\end{aligned} \tag{2.6}$$

Because $n \geq q$, $x_1, x_2 > \tau$, then $\Gamma(n-q)\int_a^t \frac{1}{(t-\tau)^{n-q-1}} > 0$
Therefore,

$$\begin{aligned}\|A_d(x_1) - A_d(x_2)\| &= \frac{1}{\Gamma(n-q)}\|\int_a^t \frac{x_1^{(n)}(\tau)}{(t-\tau)^{n-q-1}}d\tau - \int_a^t \frac{x_2^{(n)}(\tau)}{(t-\tau)^{n-q-1}}d\tau\| \\ &\leq \frac{1}{\Gamma(n-q)}\int_a^t \frac{1}{t-\tau^{n-q-1}}d\tau\|\int_a^t x_1^{(n)}(t)d\tau - \int_a^t x_2^{(n)}(t)d\tau\| \\ &\leq \frac{1}{\Gamma(n-q)}L\|x_1 - x_2\| \\ &= H\|x_1 - x_2\|\end{aligned} \tag{2.7}$$

Obviously there exists A_d which is the least constant of H.
Proof completed. □

2.3.2 Right Coprime Factorization

Operator P + Δ P : V → Y denotes a nonlinear system with uncertainties. Where P is the nominal object, ΔP means the uncertainties of object V and Y stands for the input and output space of the object.

Right factorization:

By appling an intermediate variable w ∈ W, W is called a quasi-state space of P and the input and output of the operator P are described as y = N(w) and v = D(w), respectively. If D is invertible, w(t) = D^{-1}(v)(t), then P(v(t)) = N(w(t)) = ND^{-1}(v)(t) ; if, furthermore, N and D are two stable operators, the operator P is said to have a right factorization, as shown in Figure 2.1.

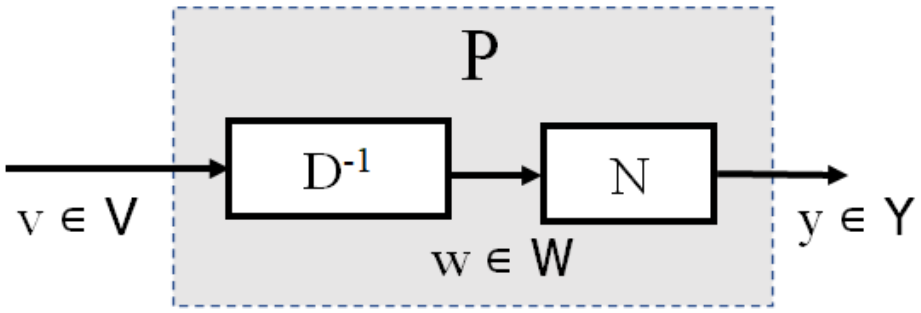

Figure 2.1: Right factorization of a nonlinear object.

Right coprime factorization:

After right factorization of a object P into (N, D), if two operators R and S satisfy the following Bezout identity, the factorization is said to be right

coprime factorization:

$$RN + SD = M \tag{2.8}$$

where R is invertible and M is a unimodular operator. The block diagram of the right coprime factorization of a nonlinear system P is shown in Figure 2.2. Figure 2.2 shows an operator-based feedback controller for a nonlinear plant P, with the operators R and S serving as the controller.

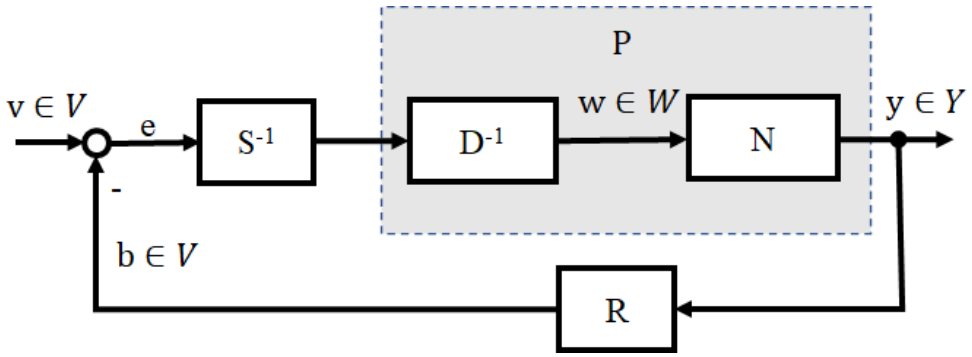

Figure 2.2: Right coprime factorization of a nonlinear system.

For a nonlinear real object $\tilde{P}$, it can be represented as a nominal object P with bounded uncertainty ΔP and $\tilde{P} = P + \Delta$. The right factorization of the nominal object P and the overall object $\tilde{P}$ are

$$P = ND^{-1} \tag{2.9}$$

and

$$P + \Delta P = (N + \Delta N)D^{-1} \tag{2.10}$$

where N, ΔN, and D are stable operators, D is invertible, and ΔN is unknown while the upper and lower bounds are known. If the following Bezout identity

is satisfied and if $\tilde{M}$ is a unimodular operator, then the nonlinear feedback control system is said to be BIBO stable.

$$R(N + \Delta N) + SD = \tilde{M} \tag{2.11}$$

With the operators S and R determined, if they further satisfy the following condition then the robustness of the uncertain system is guaranteed:

$$\|R((N + \Delta N) - RN)M^{-1}\|_{Lip} < 1 \tag{2.12}$$

where $\| \bullet \|_{Lip}$ is a Lipschitz operator norm. The robust operator-based feedback control system with uncertainty is shown in Figure 2.3.

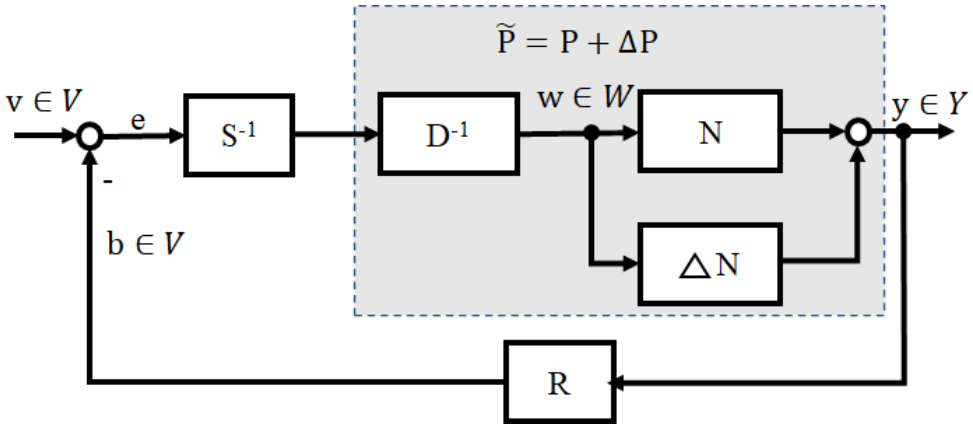

Figure 2.3: Nonlinear operator-based feedback control system with uncertainty.

Theorem 2 ([72]). *Let D^e be a linear subspace of the extended linear space U^e associated with a given Banach space U_B, and let $(R(N + \Delta N) + RN)M^{-1} \in Lip(D^e)$. Let the Bezout identity of the nominal plant and the exact plant be $RN + SD = M \in \mathcal{U}(W, U)$, $R(N + \Delta N) + SD = \tilde{M}$, respectively. If*

$$\|(R(N + \Delta N) - RN)M^{-1}\| < 1 \tag{2.13}$$

then the system shown in Figure 2.3 is robust stable for ΔN.

Theorem 3 ([72]). *Let D^e be a linear subspace of the extended linear space U^e associated with a given Banach space U_B, and let $(R(N+\Delta N)-RN+S(D+\Delta D)-SD)M^{-1} \in Lip(D^e)$. Let the Bezout identity of the nominal plant and the exact plant be $RN+SD=M \in \mathcal{U}(W,U)$, $R(N+\Delta N)+S(D+\Delta D)=\tilde{M}$, respectively. If*

$$\|(R(N+\Delta N)-RN+S(D+\Delta D)-SD)M^{-1}\|<1 \tag{2.14}$$

then the system shown in Figure 2.4 is robust stable for $\Delta N, \Delta D$.

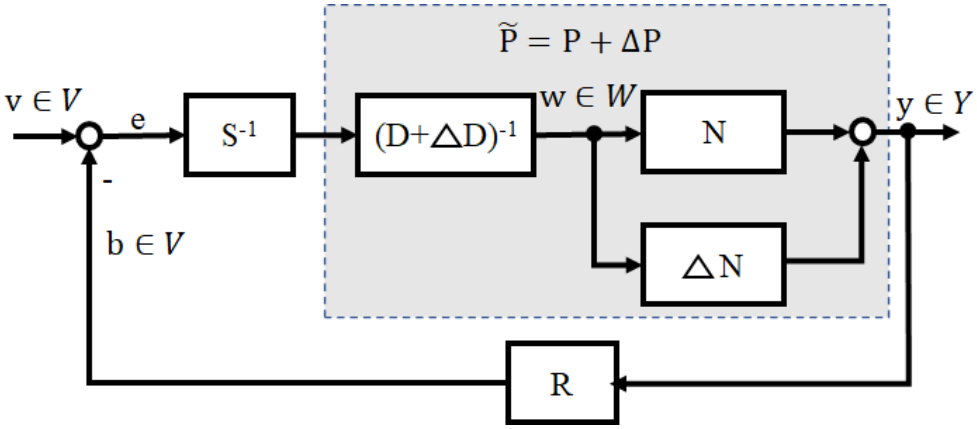

Figure 2.4: Nonlinear operator-based feedback control system with uncertainties.

Theorem 4. *Let D^e be a linear subspace of the extended linear space U^e associated with a given Banach space U_B, and let $(R(N+\Delta N)-RN+SD)M^{-1} \in Lip(D^e)$. Let the Bezout identity of the nominal plant and the exact plant be $RN+SD=M \in \mathcal{U}(W,U)$, $R(N+\Delta N)+SD=\tilde{M}$, respectively. If*

$$\|R(N+\Delta N)-RN\|<\frac{1}{\|M^{-1}\|} \tag{2.15}$$

then the system shown in Figure 2.3 is robust stable for ΔN.

Proof.

$$\|(R(N+\Delta N)-RN)M^{-1}\| < \|R(N+\Delta N)-RN\|\|M^{-1}\| \tag{2.16}$$

If

$$\|R(N+\Delta N)-RN\| < \frac{1}{\|M^{-1}\|} \tag{2.17}$$

then

$$\|(R(N+\Delta N)-RN)M^{-1}\| < 1 \tag{2.18}$$

According to Theorem 2, the system shown in Figure 2.3 is robust stable for ΔN.
Proof completed. □

Theorem 5. *Let D^e be a linear subspace of the extended linear space U^e associated with a given Banach space U_B, and let $(R(N+\Delta N)-RN+S(D+\Delta D)-SD)M^{-1} \in Lip(D^e)$. Let the Bezout identity of the nominal plant and the exact plant be $RN+SD=M \in \mathcal{U}(W,U)$, $R(N+\Delta N)+S(D+\Delta D)=\tilde{M}$, respectively. If the condition*

$$\|R(N+\Delta N)-RN+S(D+\Delta D)-SD\| < \frac{1}{\|M^{-1}\|} \tag{2.19}$$

is satisfied, then the system shown in Figure 2.4 is robustly stable for ΔN, ΔD.

Proof. In the same method with Theorem 4, this theorem was proved. □

2.4 Particle Swarm Optimization

Particle swarm optimization (PSO) is a population-based stochastic optimization technique developed by Eberhart and Kennedy in 1995, inspired by the

social behavior of bird flocking or fish schooling [89]. PSO shares many similarities with evolutionary computation techniques such as genetic algorithms (GA) and ant colony optimization (ACO) algorithms [90]. The system is initialized with a population of random solutions and searches for optima by updating iterations. However, unlike GA, PSO has no evolution operators such as crossover and mutation [91]. In PSO, potential solutions, called particles, fly through the problem space by following the current optimum particles.

It has been successfully applied to many problems in several fields such as biomedicine and energy conversion. Image analysis is one of the most frequent applications and it has been performed on biomedical images, microwave imaging, among others.

2.5 Problem statement

In this dissertation, a spiral heat exchanger is a nonlinear system with many uncertainties. In many applications, the output temperature of cooled or heated side is diffficult to control for many disturbances and complex working cinditions. The difficulty is to deal with the uncertain ties. So, a suitable closed-loop control method is proposed to realize the output temperature of a spiral heat exchanger to deal with such problem.

Firstly, A parallel fractional order derivative model and the problem statement are introduced. Then, the fractional order derivative model for the spiral-plate heat exchanger is constructed by mathematic analysis and extending from classical integer order derivative. Further, the parallel fractional order derivative model for the spiral-plate heat exchanger is constructed by considering the merit of GPU. Finally, the parallel fractional order derivative model for the spiral-plate heat exchanger is simulated. Simulations show the relationships between the output temperature of heated fluid and the

fractional orders of the two fluids, the input volume flow rate of cold fluid, and the input volume flow rate of cold fluid, respectively.

Secondly, this dissertation studies operator & fractional order nonlinear robust control for a spiral counter-flow heat exchanger with uncertainties and disturbances. First, statement problem about nonlinear fractional order derivative equation with uncertainties is described. Then, operator fractional order controller and fractional order PID controller are6 designed and some parameters are determined. Simulations verify tracking and anti-disturbance performance by comparison of different control cases.

Thirdly, nonlinear robust control for the spiral heat exchanger based on operator and FOPID described by parallel fractional order model is proposed. The parallel fractional order model for the spiral heat exchanger is identified by PSO. FOPID controller and operator controller for the spiral heat exchanger are designed under parallel fractional order mathematical model. The parameters of FOPID controller are optimized by PSO. Comparisons of two control cases are performed, and the effectiveness is illustrated.

In summary, this dissertation proposes parallel fractional order derivative model and operator & fractional order nonlinear robust control for the spiral counter-flow heat exchanger with uncertainties under disturbances.

2.6 Conclusion

In this chapter, the fractioal order preliminaries and operator theoretical background to remaining the following chapters of this dissertation is given. In addition, the problems which is discussed in this dissertation are stated, which gives the framework of our work.

Chapter 3

GPU Based Modelling and Analysis of Parallel Fractional Order Model for the Spiral-Plate Heat Exchanger plant

3.1 Introduction

In this chapter, a parallel fractional order derivation model is proposed by considering the merit of the graphics processing unit (GPU). Then, the parallel fractional order derivation model for the spiral-plate heat exchanger is constructed. Simulations show the relationships between the output temperature of heated fluid and the orders of fractional order derivatives with two directional fluids impacted by complex factors, namely, the volume flow rate in hot fluid, and the volume flow rate in cold fluid, respectively. In Section 3.2, a parallel fractional order derivative model is proposed.

In Section 3.3, a mathematic fractional order derivative model for the spiral-plate heat exchanger is derived.

In Section 3.4, the proposed parallel model for the spiral-plate heat

exchanger with both the counter-flow type and the parallel-flow type and implementation on GPU are given.

Section 3.5 compares the relationships between the output temperature of the heated flow fluid and the orders of the fractional order derivative with the two directional fluids, the volume flow rate of cold fluid, and the volume flow rate of hot fluid, respectively

Finally, in Section 3.6, a conclusion is given.

3.2 Parallel Fractional Order Derivative Model

In reference [42], parallel fractional order derivative model is not complete only modelling of a spiral heat exchanger with counter-type by using fractional order equation and without theory support. It is richened to derive this paper.

According to the definition of the fractional order derivative, the fractional order derivative Equation (3.1) are given as follows.

$$\begin{cases} D_t^q f(\Delta h) = \quad -(\Delta h)^{-q}\frac{\Gamma(q+1)}{\Gamma(2)\Gamma(q)}f(0) + (\Delta h)^{-q}f(\Delta h) \\ D_t^q f(2(\Delta h)) = (\Delta h)^{-q}\frac{\Gamma(q+1)}{\Gamma(3)\Gamma(q-1)}f(0) - (\Delta h)^{-q}\frac{\Gamma(q+1)}{\Gamma(2)\Gamma(q)}f(\Delta h) + (\Delta h)^{-q}f(2(\Delta h)) \\ D_t^q f(3(\Delta h)) = -(\Delta h)^{-q}\frac{-\Gamma(q+1)}{\Gamma(4)\Gamma(q-2)}f(0) + (\Delta h)^{-q}\frac{\Gamma(q+1)}{\Gamma(3)\Gamma(q-1)}f(\Delta h) \\ \qquad\qquad\qquad -(\Delta h)^{-q}\frac{\Gamma(q+1)}{\Gamma(2)\Gamma(q)}f(2(\Delta h)) + (\Delta h)^{-q}f(3(\Delta h)) \\ \qquad \vdots \\ D_t^q f(N(\Delta h)) = (\Delta h)^{-q}\sum_{j=1}^{N}(-1)^j\frac{\Gamma(q+1)}{\Gamma(j+1)\Gamma(q-j+1)}f(t-j(\Delta h)) + (\Delta h)^{-q}f(N(\Delta h)) \end{cases} \tag{3.1}$$

From (3.1), a parallel fractional order derivative model is described by the matrix, as follow.

$$F_k = (\Delta h)^q D_{frac} + BF_{k-1} \tag{3.2}$$

where F_k, F_{k-1}, $D_{frac} \in R^N$, and $B \in R^{N \times N}$

$$F_k = \begin{pmatrix} f(\Delta h) \\ f(2(\Delta h)) \\ \vdots \\ f(N(\Delta h)) \end{pmatrix} \tag{3.3}$$

$$D_{frac} = \begin{pmatrix} D_t^q f(\Delta h) \\ D_t^q f(2(\Delta h)) \\ \vdots \\ D_t^q f(N(\Delta h)) \end{pmatrix} \tag{3.4}$$

$$B = \begin{pmatrix} \frac{-\Gamma(q+1)}{\Gamma(2)\Gamma(q)} & 0 & \cdots & 0 \\ \frac{\Gamma(q+1)}{\Gamma(3)\Gamma(q-1)} & \frac{-\Gamma(q+1)}{\Gamma(2)\Gamma(q)} & \cdots & 0 \\ \vdots & \vdots & \vdots & \vdots \\ \frac{(-1)^N\Gamma(q+1)}{\Gamma(N+1)\Gamma(q-N+1)} & \frac{(-1)^{(N-1)}\Gamma(q+1)}{\Gamma(N)\Gamma((q-N+1)} & \cdots & \frac{-\Gamma(q+1)}{\Gamma(2)\Gamma(q)} \end{pmatrix} \tag{3.5}$$

$$F_{k-1} = \begin{pmatrix} f(0) \\ f(\Delta h) \\ \vdots \\ f((N-1)(\Delta h)) \end{pmatrix} \tag{3.6}$$

3.3 Mathematics analysis

3.3.1 Fractional order derivative model for the spiral-plate counter-flow heat exchanger

In this section, the spiral-plate heat exchanger with the counter-flow type is analyzed here. First, we consider the temperature variable in cold fluid, that is divided into a micro volume as shown in Figure 3.1. Here, v_h is the flow rate in hot fluid. v_c is the flow rate in cold fluid. The directions of v_h, and v_c are opposite. ΔV is a micro volume in cold fluid. Δm_1 is the heat flux

transferring from the inside $T_h(x)$. Δm_2 is the heat flux transferring from the outside $T_h(x + C)$, C is the length to the angle of 2π.

As seen in Figure 3.1, it denotes the heat transferring between the two fluids for the spiral-plate counter-flow heat exchanger.

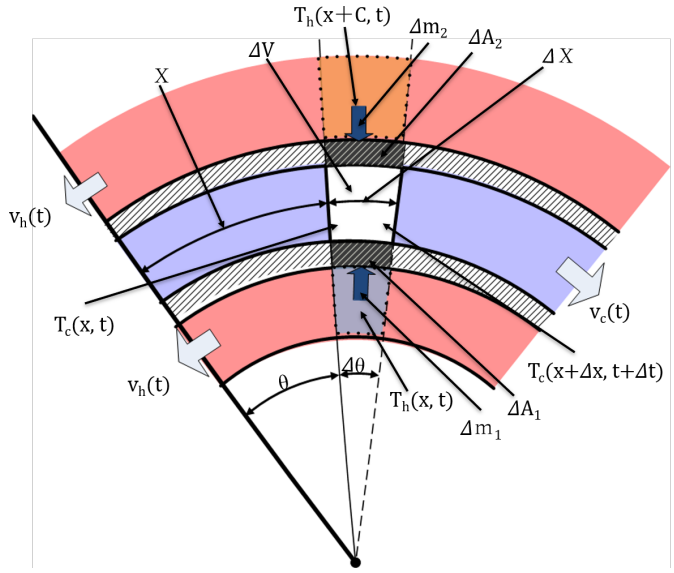

Figure 3.1: The principle of heat transfer for the spiral heat exchanger.

Therefore, according to the heat energy balance law and heat transfer theory [44], the equations are derived as follows.

$$c_c \rho_c (\Delta V) \frac{\Delta T_c(x,t)}{\Delta t} = \Delta m_1 + \Delta m_2 \tag{3.7}$$

$$\frac{\Delta T_c(x,t)}{\Delta t} = T_c(x + \Delta x, t + \Delta t) - T_c(x,t) \tag{3.8}$$

Where c_c, ρ_c, ΔV, k is the specific heat capacity of cold fluid, the density of cold fluid, a micro volume, the heat transfer coefficient of the spiral-plate

heat exchanger, respectively. According to the Newton's law of cooling.

$$k = \frac{1}{h_h} + \frac{\delta_s}{\lambda} + \frac{1}{h_c} \tag{3.9}$$

Where h_h, h_c, δ_s, and λ is the heat transfer coefficient of hot fluid, the heat transfer coefficient of cold fluid, the width of wall, thermal conductivity, respectively.

$$\Delta m_1 = k \cdot (T_h(x,t) - T_c(x,t)) \cdot (\Delta A_1) \tag{3.10}$$

Δm_1 is the heat flux transferring from $T_h(x,t)$ to $T_c(x,t)$.

Where ΔA_1 is the heat transfer suface area $T_h(x,t)$ to $T_c(x,t)$.

$$\Delta m_2 = k \cdot (T_h(x+C,t) - T_c(x,t)) \cdot (\Delta A_2) \tag{3.11}$$

Δm_2 is the heat flux transferring from $T_h(x+C,t)$ to $T_c(x,t)$.

Where ΔA_2 is the heat transfer surface area $T_h(x+C,t)$ to $T_c(x,t)$. Each element is of the length Δx and the heat transfer surface area $\Delta A_1, \Delta A_2$, and $\Delta A_1 \approx \Delta A_2 = \Delta A = (\Delta x) \cdot Z$, Z is the height of the spiral-plate heat exchanger, Δx is the displacement of cold fluid that moves in time Δt, $\Delta V = (\Delta x) \cdot Z \cdot \delta_h$, $\Delta t = \dfrac{\Delta x}{v_c}$. So,

$$c_c \rho_c \delta_c v_c \frac{\Delta T_c(x,t)}{\Delta x} = k(T_h(x,t) + T_h(x+C,t) - 2T_c(x,t)) \tag{3.12}$$

Using the thought of differential theory, the relationship between the length in the differential arc and the angle in differential arc is derived.

$$\Delta x = \sqrt{\Delta r^2 + (r(\Delta\theta))^2} \tag{3.13}$$

Applying the spiral function of the spiral-plate heat exchanger, $r = a\theta + b$, it is obtained from (3.13):

$$\Delta x = \sqrt{a^2 + (b + a\theta)^2}(\Delta\theta) \tag{3.14}$$

Substituting (3.14) into (3.12), the differential equation in cold fluid is obtained as follow.

$$c_c\rho_c\delta_c v_c\frac{\Delta T_c(\theta,t)}{\Delta\theta} = k\sqrt{a^2+(b+a\theta)^2}(T_h(\theta,t)+T_h(\theta+2\pi,t)-2T_c(\theta,t)), \theta\in[0,11\pi) \tag{3.15}$$

Because (3.15) is complex. we simplify (3.16) as follow.

$$c_c\rho_c\delta_c v_c\frac{\Delta T_c(\theta,t)}{\Delta\theta} = Fk\sqrt{a^2+(b+a\theta)^2}(T_h(\theta,t)-T_c(\theta,t)), \theta\in[0,11\pi) \tag{3.16}$$

Where F is the constant between 1 and 2 relation to the shape of the heat exchanger. According to the thought of fractional order derivative [15] (3.16) is extended from the integer order derivative to the fractional order derivative, we derive fractional order derivative equation in cold fluid for the spiral-plate counter-flow heat exchanger as follow. Here, fractional order is impacted by complex factors, it is difficult to derive by theory method.

$$c_c\rho_c\delta_c v_c D_\theta^{q_2}T_c(\theta,t) = Fk\sqrt{a^2+(b+a\theta)^2}(T_h(\theta,t)-T_c(\theta,t)), \theta\in[0,11\pi) \tag{3.17}$$

With the same principle, the fractional order derivative equation in hot fluid is derived as follow.

$$c_h\rho_h\delta_h v_h D_\theta^{q_1}T_h(\theta,t) = Fk\sqrt{a^2+(b+a\theta)^2}(T_c(\theta,t)-T_h(\theta,t)), \theta\in[0,11\pi) \tag{3.18}$$

$$A = \sqrt{a^2+(b+a\theta)^2} \tag{3.19}$$

Nonlinear fractional order derivative equations for the spiral-plate counter-flow heat exchanger are given as follows.

$$\begin{cases} D_\theta^{q_1}T_h(\theta,t) = \dfrac{kFA}{v_h c_h\rho_h\delta_h}((T_c(\theta,t)-T_h(\theta,t)) \\ D_\theta^{q_2}T_c(\theta,t) = \dfrac{kFA}{v_c c_c\rho_c\delta_c}((T_h(\theta,t)-T_c(\theta,t)) \\ \theta\in[0,11\pi] \end{cases} \tag{3.20}$$

Where $v_h(t)$ and $v_c(t)$ is the input flow rate of time t in hot fluid, the input flow rate of time t in cold fluid side, respectively.

$$\begin{cases} QL_1 = \delta_h Z v_h \\ QL_2 = \delta_c Z v_c \end{cases} \tag{3.21}$$

Where QL_1 and QL_2 is the input volume flow rate in hot fluid side and the input volume flow rate in cold fluid side, respectively.

Substituting (3.21) into (3.20), fractional order derivative model for the spiral-plate counter-flow heat exchanger is described as follow.

$$\begin{cases} D_\theta^{q_1} T_h(\theta, t) = \dfrac{kFAZ}{QL_1 c_h \rho_h}((T_c(\theta, t) - T_h(\theta, t)) \\ D_\theta^{q_2} T_c(\theta, t) = \dfrac{kFAZ}{QL_2 c_c \rho_c}((T_h(\theta, t) - T_c(\theta, t)) \\ \theta \in [0, 11\pi] \end{cases} \tag{3.22}$$

Considering boundary conditions, $T_h(11\pi, t)$ and $T_c(0, t)$ is the input temperature of time t in hot fluid, the input temperature of time t in cold fluid, respectively.

3.3.2 Fractional order derivative model for the spiral-plate parallel-flow heat exchanger

With the same method, the fractional order derivative model for the spiral-plate parallel-flow heat exchanger is derived as follow.

$$\begin{cases} D_\theta^{q_1} T_h(\theta, t) = \dfrac{kFAZ}{QL_1 c_h \rho_h}((T_c(\theta, t) - T_h(\theta, t)) \\ D_\theta^{q_2} T_c(\theta, t) = \dfrac{kFAZ}{QL_2 c_c \rho_c}((T_h(\theta, t) - T_c(\theta, t)) \\ \theta \in [0, 11\pi] \end{cases} \tag{3.23}$$

Considering boundary conditions, $T_h(0, t)$ and $T_c(0, t)$ is the input temperature of time t in hot fluid, the input temperature of time t in cold fluid side, respectively.

The fractional order derivation equations for the spiral-plate parallel-flow heat exchanger are similar to that with the spiral-plate counter-flow heat exchanger, but the boundary conditions are different.

3.4 Parallel fractional order derivative model for the spiral-plate heat exchanger

3.4.1 Parallel model for the spiral-plate counter-flow heat exchanger

Applying (3.1) - (3.6) into (3.22), parallel fractional order derivative model for the spiral-plate counter-flow heat exchanger is described as follow.

$$\begin{cases} T_{hk} = (\Delta\theta)^{q_1} D_{hfrac} + B_h T_{hk-1} \\ T_{ck} = (\Delta\theta)^{q_2} D_{cfrac} + B_c T_{ck-1} \end{cases} \tag{3.24}$$

Where $T_{hk}, T_{hk-1}, D_{hfrac} \in R^N$, and $B_h \in R^{N\times N}$
$T_{ck}, T_{ck-1}, D_{cfrac} \in R^N$, and $B_c \in R^{N\times N}$

$$T_{hk} = \begin{pmatrix} T_h(\Delta\theta) \\ T_h(2(\Delta\theta)) \\ \vdots \\ T_h(N(\Delta\theta)) \end{pmatrix} \tag{3.25}$$

$$B_h = \begin{pmatrix} \frac{-\Gamma(q_1+1)}{\Gamma(2)\Gamma(q_1)} & 0 & \cdots & 0 \\ \frac{\Gamma(q_1+1)}{\Gamma(3)\Gamma(q_1-1)} & \frac{-\Gamma(q_1+1)}{\Gamma(2)\Gamma(q_1)} & \cdots & 0 \\ \vdots & \vdots & \vdots & \vdots \\ \frac{(-1)^N\Gamma(q_1+1)}{\Gamma(N+1)\Gamma(q_1-N+1)} & \frac{(-1)^{(N-1)}\Gamma(q_1+1)}{\Gamma(N)\Gamma((q_1-N+1)} & \cdots & \frac{-\Gamma(q_1+1)}{\Gamma(2)\Gamma(q_1)} \end{pmatrix} \tag{3.26}$$

$$T_{hk-1} = \begin{pmatrix} T_h(0) \\ T_h(\Delta\theta) \\ \vdots \\ T_h((N-1)(\Delta\theta)) \end{pmatrix} \tag{3.27}$$

$$B_c = \begin{pmatrix} frac-\Gamma(q_2+1)\Gamma(2)\Gamma(q_2) & 0 & \cdots & 0 \\ \frac{\Gamma(q_2+1)}{\Gamma(3)\Gamma(q_2-1)} & \frac{-\Gamma(q_2+1)}{\Gamma(2)\Gamma(q_2)} & \cdots & 0 \\ \vdots & \vdots & \vdots & \vdots \\ \frac{(-1)^N\Gamma(q_2+1)}{\Gamma(N+1)\Gamma(q_2-N+1)} & \frac{(-1)^{(N-1)}\Gamma(q_2+1)}{\Gamma(N)\Gamma((q_2-N+1)} & \cdots & \frac{-\Gamma(q_2+1)}{\Gamma(2)\Gamma(q_2)} \end{pmatrix} \tag{3.28}$$

$$T_{ck} = \begin{pmatrix} T_c(\Delta\theta) \\ T_c(2\Delta\theta) \\ \vdots \\ T_c(N(\Delta\theta)) \end{pmatrix} \tag{3.29}$$

$$T_{ck-1} = \begin{pmatrix} T_c(0) \\ T_c(\Delta\theta) \\ \vdots \\ T_c((N-1)(\Delta\theta)) \end{pmatrix} \tag{3.30}$$

So, the parallel fractional order derivative model for the spiral-plate counter-flow heat exchanger is obtained.

$$\begin{cases} T_{hk} = (\Delta\theta)^{q_1}\dfrac{FkZA}{QL_1c_h\rho_h}(HT_{cK-1} - T_{hK-1}) + B_hT_{hk-1} \\ T_{ck} = (\Delta\theta)^{q_2}\dfrac{FkZA}{QL_2c_c\rho_c}(HT_{hK-1} - T_{cK-1}) + B_cT_{ck-1} \\ T_{cout} = CT_{ck} \end{cases} \tag{3.31}$$

$$\begin{cases} D_{hfrac} = \dfrac{FkZA}{QL_1c_h\rho_h}(HT_{cK-1} - T_{hK-1}) \\ D_{cfrac} = \dfrac{FkZA}{QL_2c_c\rho_c}(HT_{hK-1} - T_{cK-1}) \end{cases} \tag{3.32}$$

$$\begin{cases} T_{hk} = (\Delta\theta)^{q_1} D_{hfrac} + B_h T_{hk-1} \\ T_{ck} = (\Delta\theta)^{q_2} D_{cfrac} + B_c T_{ck-1} \end{cases} \tag{3.33}$$

Where

$$H = \begin{pmatrix} 0 & 0 & 0 & \dots & 0 & 1 \\ 0 & 0 & 0 & \dots & 1 & 0 \\ \vdots & \vdots & \vdots & \vdots & \vdots & \vdots \\ 1 & 0 & 0 & \dots & 0 & 0 \end{pmatrix} \tag{3.34}$$

$$C = \begin{pmatrix} 0 & 0 & 0 & 0 & \dots & 1 \end{pmatrix} \tag{3.35}$$

Where $C \in R^{1\times N} and H \in R^{N\times N}$. The parallel fractional order derivative model for the spiral-plate counter-flow heat exchanger is a model with the parallel input data. It has high efficiency executed on GPU. The proposed parallel model is implemented on GPU by using MATLAB and CUDA [66].

3.4.2 The proposed parallel model for the spiral-plate parallel-flow heat exchanger

The parallel fractional derivation model for the spiral-plate parallel-flow heat exchanger is obtained by the same method with the spiral-plate counter-flow heat exchanger presented as above.

With the same method from (3.22), the parallel fractional order derivative equations for the spiral-plate parallel-flow heat exchanger are described as follows.

$$\begin{cases} T_{hk} = (\Delta\theta)^{q_1} \dfrac{FkZA}{QL_1 c_1 \rho_h} (T_{cK-1} - T_{hK-1}) + B_h T_{hk-1} \\ T_{ck} = (\Delta\theta)^{q_2} \dfrac{FkZA}{QL_2 c_c \rho_c} (T_{hK-1} - T_{cK-1}) + B_c T_{ck-1} \\ T_{cout} = C T_{ck} \end{cases} \tag{3.36}$$

$$\begin{cases} D_{hfrac} = \dfrac{FkZA}{QL_1c_h\rho_h}(T_{cK-1} - T_{hK-1}) \\ D_{cfrac} = \dfrac{FkZA}{QL_2c_c\rho_c}(T_{hK-1} - T_{cK-1}) \end{cases} \tag{3.37}$$

The parallel fractional order derivative model for the spiral-plate parallel-flow heat exchanger is described as follow.

$$\begin{cases} T_{hk} = (\Delta\theta)^{q_1} D_{hfrac} + B_h T_{hk-1} \\ T_{ck} = (\Delta\theta)^{q_2} D_{cfrac} + B_c T_{ck-1} \end{cases} \tag{3.38}$$

Where T_{hk}, T_{hk-1}, $D_{hfrac} \in R^N$, and $B_h \in R^{N\times N}$
T_{ck}, T_{ck-1}, $D_{cfrac} \in R^N$, and $B_c \in R^{N\times N}$

3.5 Simulation on the proposed parallel model for the spiral-plate heat exchanger

In this section, it is analysed for the relationships between the output temperature in cold fluid and the fractional orders q_1, q_2 for the proposed parallel model for the spiral-plate heat exchanger, the volume flow rate in hot fluid and the volume flow rate in cold fluid.

Simulation parameters of the spiral-plate heat exchanger are shown in Table 4.1.

Table 3.1: Simulation parameters of the spiral-plate heat exchanger.

Meaning	Symbol	Value
The densities of the two fluids	ρ_c, ρ_h	1000 Kg/m^3
The specific heat capacity of the two fluids	c_c, c_h	4.2 $KJ/(Kg.^oC)$
The input temperature of cold fluid	$T_{c,in}$	20 ^oC
The input temperature of hot fluid	$T_{h,in}$	50 ^oC
Thermal conductivity of SUS304	λ	16.7 $W/(m^oC)$
Heat transfer coefficients of the two fluids	h_h, h_c	366 $w/m^2.K$
The orders for fractional order derivative	q_1, q_2	0.9 - 1.02
The volume flow rate of hot fluid	QL_1	1 - 7 L/min
The volume flow rate of cold fluid	QL_2	1 - 7 L/min
Correction factor	F	1.8
Simulation time	t	[0, 12] s

Table 3.3: The relateships between the output temperature of cold fluid and the flow rates of hot fluid, cold fluid for the proposed parallel model of the spiral-plate parallel-flow heat exchanger.

Figure No.	descrption
Figure 3.12	q_1, q_2 = 0.9, 0.92, 0.94, 0.96, 0.98, 1.0
Figure 3.13	q_1 , q_2 = 1.004, 1.008, 1.01, 1.02
Figure 3.14	$QL_1 = 1L/min, QL_2 = 1, 3, 5, 7L/min$
Figure 3.15	$QL_1 = 3L/min, QL_2 = 1, 3, 5, 7L/min$
Figure 3.16	$QL_1 = 5L/min, QL_2 = 1, 3, 5, 7L/min$
Figure 3.17	$QL_1 = 7L/min, QL_2 = 1, 3, 5, 7L/min$
Figure 3.18	$QL_1 = 1, 3, 5, 7L/min, QL_2 = 1L/min$
Figure 3.19	$QL_1 = 1, 3, 5, 7L/min, QL_2 = 3L/min$
Figure 3.20	$QL_1 = 1, 3, 5, 7L/min, QL_2 = 5L/min$
Figure 3.21	$QL_1 = 1, 3, 5, 7L/min, QL_2 = 7L/min$

3.5.1 Simulation on the proposed parallel model for the spiral-plate counter-flow heat exchanger

(1) Simulation with the different fractional orders as $q_1, q_2 \leq 1$.

The relationships between the output temperature in cold fluid and the

Table 3.2: The relationships between the output temperature of cold fluid and the volume flow rates of hot fluid, cold fluid for the proposed parallel model for the spiral-plate counter-flow heat exchanger.

Figure No.	descrption
Figure 3.2	q_1, q_2 = 0.9, 0.92, 0.94, 0.96, 0.98, 1.0
Figure 3.3	q_1 , q_2 = 1.004, 1.008, 1.01, 1.02
Figure 3.4	$QL_1 = 1L/min, QL_2 = 1, 3, 5, 7L/min$
Figure 3.5	$QL_1 = 3L/min, QL_2 = 1, 3, 5, 7L/min$
Figure 3.6	$QL_1 = 5L/min, QL_2 = 1, 3, 5, 7L/min$
Figure 3.7	$QL_1 = 7L/min, QL_2 = 1, 3, 5, 7L/min$
Figure 3.8	$QL_1 = 1, 3, 5, 7L/min, QL_2 = 1L/min$
Figure 3.9	$QL_1 = 1, 3, 5, 7L/min, QL_2 = 3L/min$
Figure 3.10	$QL_1 = 1, 3, 5, 7L/min, QL_2 = 5L/min$
Figure 3.11	$QL_1 = 1, 3, 5, 7L/min, QL_2 = 7L/min$

fractional orders as $q_1, q_2 \leq 1$ are shown in Figure 3.2. Those show that the output temperature increases with the fractional orders q_1, q_2 rises up as shown in Figure 3.2.

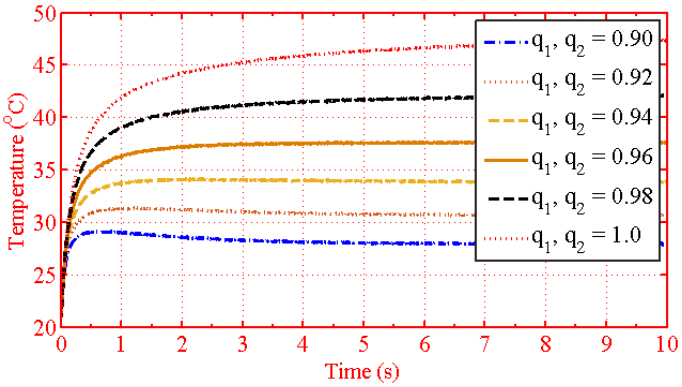

Figure 3.2: The output temperature in cold fluid as q_1, $q_2 \leq 1$.

(2) Simulation with the different fractional orders as q_1, $q_2 > 1$.

The relationships between the output temperature in cold fluid and the

different fractional orders as q_1, $q_2 > 1$ are shown in Figure 3.3. It shows when q_1, $q_2 = 1.025$, the output temperature in cold fluid is unstable.

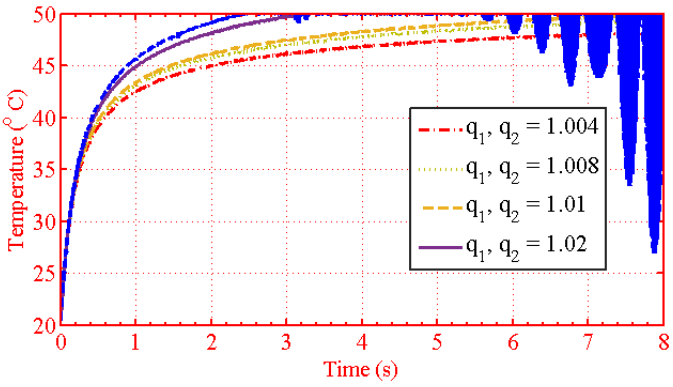

Figure 3.3: The output temperature in cold fluid as q_1, $q_2 > 1$.

(3) The relationships between the output temperature in cold fluid and the different volume flow rate of hot fluid.

The relationships between the output temperature in cold fluid and the different volume flow rate of hot fluid are shown in Figures 3.4 - 3.7. Those figures show that the output temperature rises with the volume flow rate of hot fluid increases.

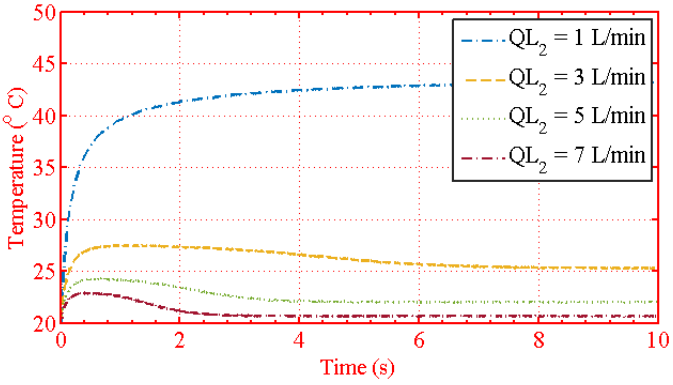

Figure 3.4: The output temperature in cold fluid with $QL_1 = 1$ L/Min.

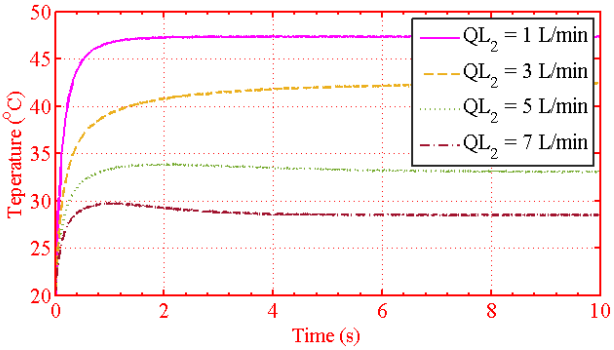

Figure 3.5: The output temperature in cold fluid with $QL_1 = 3$ L/Min.

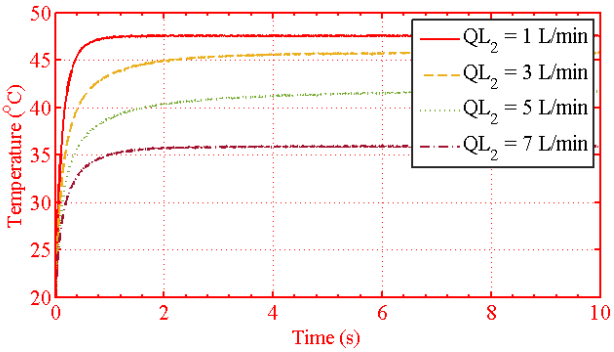

Figure 3.6: The output temperature in cold fluid with $QL_1 = 5$ L/Min.

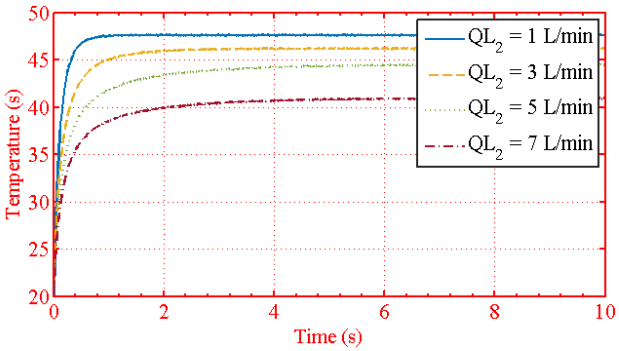

Figure 3.7: The output temperature in cold fluid with $QL_1 = 7$ L/Min.

(4) The relationships between the output temperature in cold fluid and the different volume flow rate of cold fluid.

The relationships between the output temperature in cold fluid and the different volume flow rate of cold fluid are shown in Figures 3.8 - 3.11. Those figures show that the output temperature in cold fluid goes down with the volume flow rate of cold fluid increases.

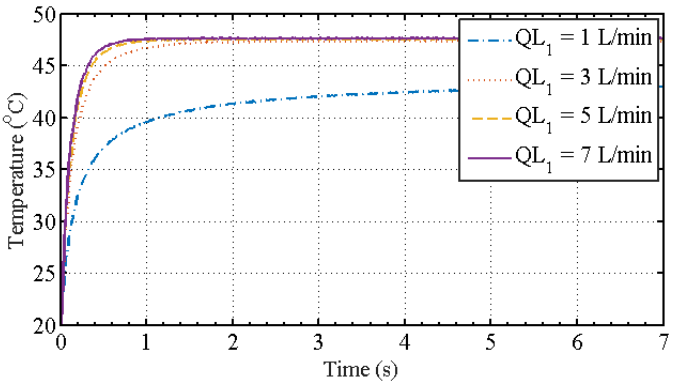

Figure 3.8: The output temperature in cold fluid with $QL_2 = 1$ L/Min.

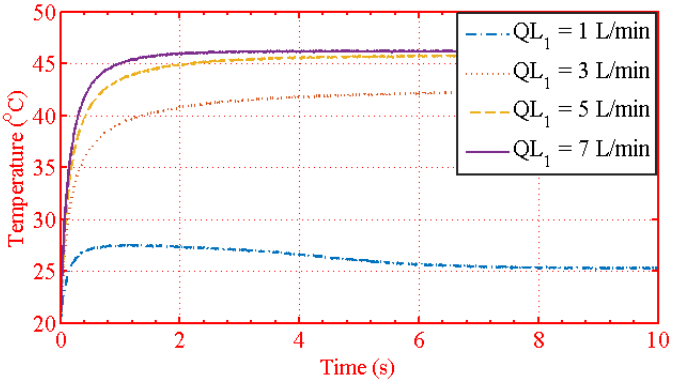

Figure 3.9: The output temperature in cold fluid with $QL_2 = 3$ L/Min.

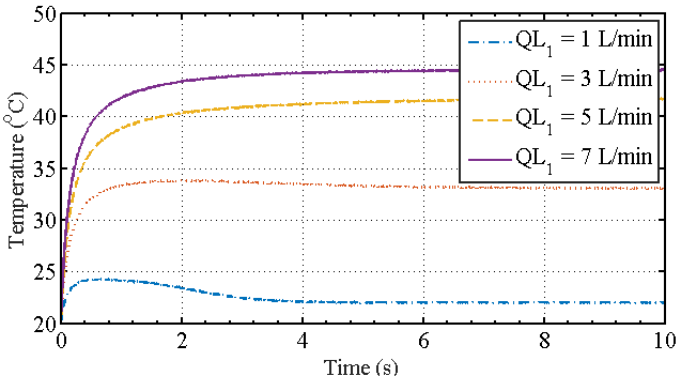

Figure 3.10: The output temperature in cold fluid with $QL_2 = 5$ L/Min.

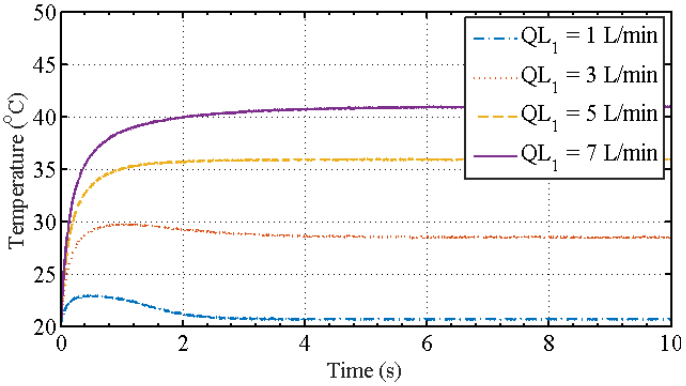

Figure 3.11: The output temperature in cold fluid with $QL_2 = 7$ L/Min.

3.5.2 Simulation on the proposed parallel model for the spiral-plate parallel-flow heat exchanger

In this section, it is analysed for the relationships between the output temperature in cold fluid, the fractional orders q_1, q_2 , the volume flow rate of hot fluid, and the volume flow rate of cold fluid. Simulation parameters are given in Table 4.1.

(1) Simulation with the different fractional orders as $q_1, q_2 \leq 1$.

The relationships between output temperature in cold fluid and the fractional orders as $q_1, q_2 \leq 1$ are shown in Figure 3.12. They show that the output temperature rises with the fractional orders q_1, q_2 increases as shown in Figure 3.12.

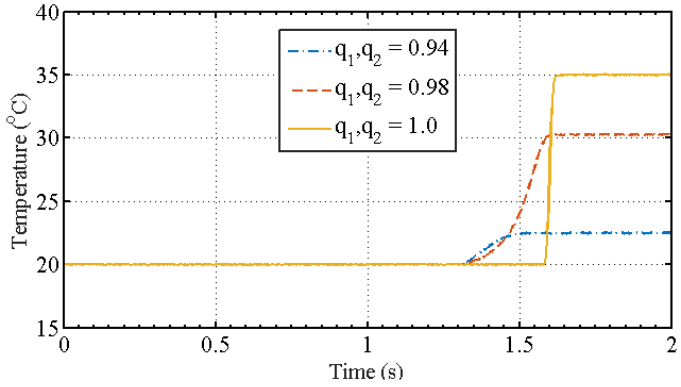

Figure 3.12: The output temperature in cold fluid as q_1, $q_2 \leq 1$.

(2) Simulation with the different fractional orders as q_1, $q_2 > 1$.

The relationships between the output temperature in cold fluid and the fractional orders as q_1, $q_2 > 1$ are shown in Figure 3.13. When q_1, q_2 is 1.025, the output temperature in cold fluid is unstable.

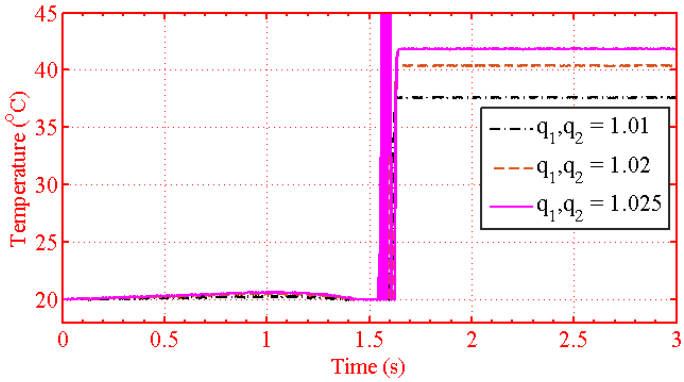

Figure 3.13: The output temperature in cold fluid as q_1, $q_2 > 1$.

(3) The relationships between the output temperature of cold fluid and the different volume flow rate of hot fluid.

The relationships between the output temperature in cold fluid and the different volume flow rate of hot fluid are shown in Figures 3.14 - 3.17. Those figures show that output temperature in cold fluid rises with the volume flow rate of hot fluid increases.

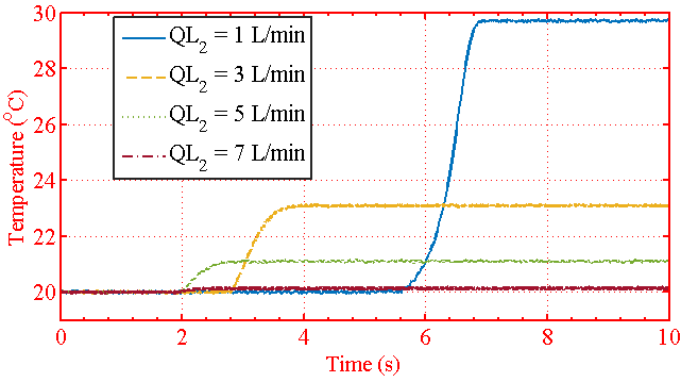

Figure 3.14: The output temperature in cold fluid with $QL_1 = 1$ L/Min.

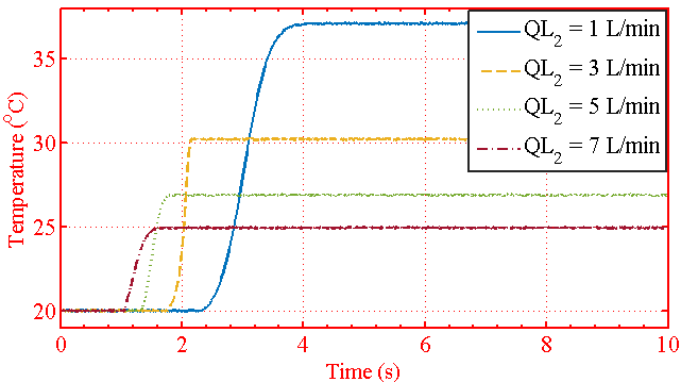

Figure 3.15: The output temperature in cold fluid with $QL_1 = 3$ L/Min.

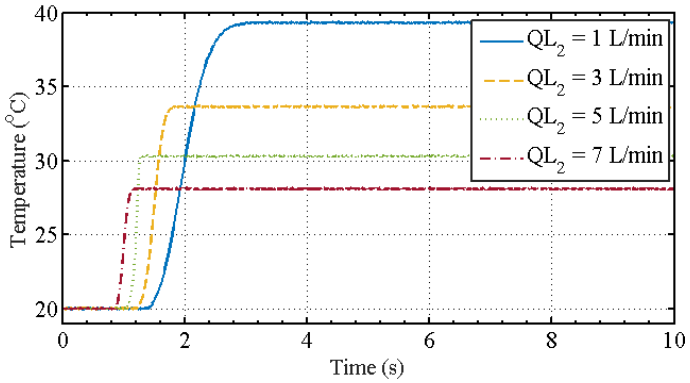

Figure 3.16: The output temperature in cold fluid with $QL_1 = 5$ L/Min.

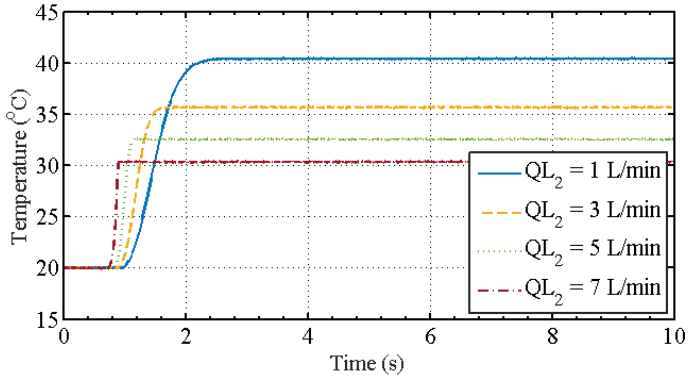

Figure 3.17: The output temperature in cold fluid with $QL_1 = 7$ L/Min.

(4) The relationships between the output temperature of cold fluid and the different volume flow rate of cold fluid.

The relationships between the output temperature in cold fluid and the different volume flow rate of cold fluid are shown in Figures. 3.18 - 3.21. Those figures show that the output temperature in cold fluid drops down with the volume flow rate of cold fluid increases.

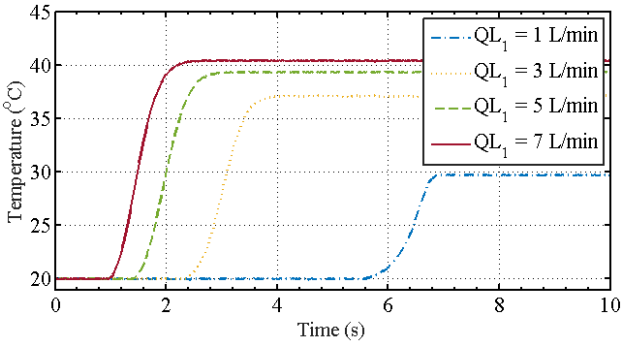

Figure 3.18: The output temperature in cold fluid with $QL_2 = 1$ L/Min.

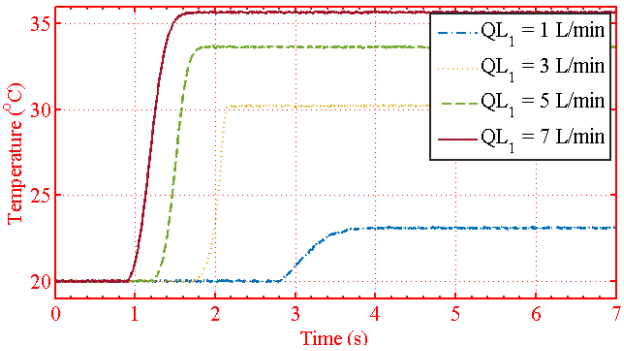

Figure 3.19: The output temperature in cold fluid with $QL_2 = 3$ L/Min.

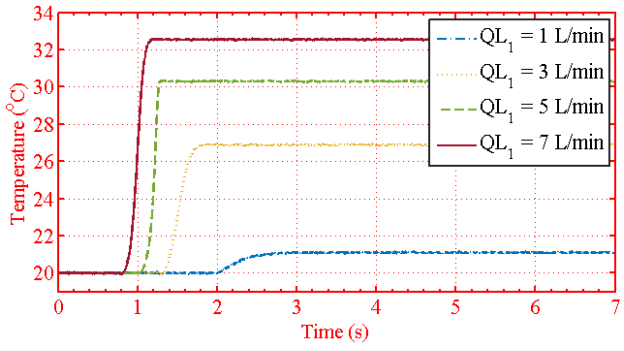

Figure 3.20: The output temperature in cold fluid with $QL_2 = 5$ L/Min.

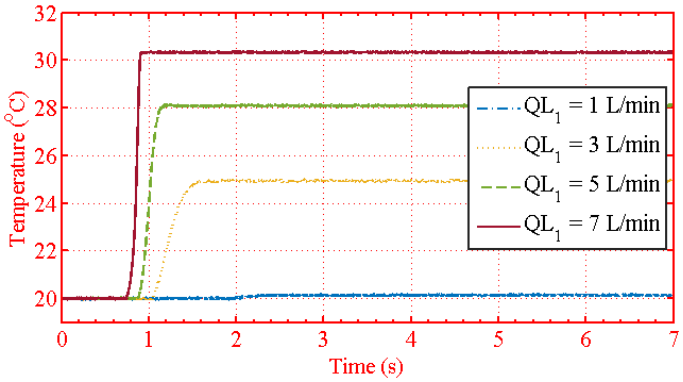

Figure 3.21: The output temperature in cold fluid with $QL_2 = 7$ L/Min.

3.6 Conclusion

A parallel fractional order derivative model and the problem statement are introduced in this paper. Then, the fractional order derivative model for the spiral-plate heat exchanger is constructed by mathematic analysis and extending from classical integer order derivative. Further, the parallel fractional order derivative model for the spiral-plate heat exchanger is constructed by considering the merit of GPU. Finally, the parallel fractional order derivative model for the spiral-plate heat exchanger is simulated. Simulations show the relationships between the output temperature of heated fluid and the fractional orders of the two fluids, the input volume flow rate of cold fluid, and the input volume flow rate of cold fluid, respectively.

Chapter 4

Operator & Fractional Order Based Nonlinear Robust Control for the Spiral Heat Exchanger

4.1 Introduction

This chapter studies operator and fractional order nonlinear robust control for a spiral counter-flow heat exchanger with uncertainties and disturbances. The design of an operator fractional order controller and fractional order PID controller and determination of several related parameters is described. Simulations were performed to verify tracking and anti-disturbance performance by comparison to different control cases; verification is described and concluding remarks provided.

In Section 4.2 a problem statement concerning fractional order equations for a spiral-plate heat exchanger is presented.

In Section 4.3, a fractional order operator controller is designed and the different control cases are analyzed in terms of tracking performance and stability.

Simulations verifying operator and fractional order-based robust nonlinear control for a spiral counter-flow heat exchanger with uncertainties and disturbances are reviewed in Section 4.4.

In Section 4.5 conclusions are provided.

4.2 Fractional order equation for a spiral heat exchanger

According to the law of heat-energy balance of two fluids, the fractional order derivative model for a spiral-plate parallel flow heat exchanger is derived as follows [46]:

$$\begin{cases} D_\theta^{q_1} T_h(\theta,t) = \dfrac{(k+\Delta k)FAZ}{QL_1 c_h \rho_h}(T_c(\theta,t) - T_h(\theta,t) \\ D_\theta^{q_2} T_c(\theta,t) = \dfrac{(k+\Delta k)FAZ}{QL_2 c_c \rho_c}(T_h(\theta,t) - T_c(\theta,t) \\ \theta \in [0, 11\pi] \end{cases} \tag{4.1}$$

Let $q_1 = q$, $q_2 = q + \Delta q$, then,

$$\begin{aligned} D_\theta^{q_2} T_c(\theta,t) &= D_\theta^q T_c(\theta,t) - \Delta D_q \\ &= \frac{kFAZ}{QL_2 c_c \rho_c}(T_h(\theta,t) - T_c(\theta,t)) \end{aligned} \tag{4.2}$$

Thus,

$$D_\theta^q T_h(\theta,t) = \frac{(k+\Delta k)FAZ}{QL_1 k_h}(T_c(\theta,t) - T_h(\theta,t)) \tag{4.3}$$

$$D_\theta^q T_c(\theta,t) + \Delta D_q = \frac{(k+\Delta k)FAZ}{QL_2 k_c}(T_h(\theta,t) - T_c(\theta,t)) \tag{4.4}$$

$$\theta \in [0, 11\pi]$$

$$D_\theta^q(\Delta T(\theta,t)) + \Delta D_q = FAZ(\frac{1}{k_c Q L_2} + \frac{1}{k_h Q L_1})\Delta T(\theta,t) \tag{4.5}$$

where $k = \frac{\delta_s}{\lambda}$, $k + \Delta k = \frac{1}{h_h} + \frac{\delta_s}{\lambda} + \frac{1}{h_c}$, $k_c = c_c\rho_c$, $k_h = c_h\rho_h$, and $\Delta T(\theta,t)$ $= T_c(\theta,t) - T_h(\theta,t)$. $A = \sqrt{a^2+b^2}$ and $A + \Delta A = \sqrt{a^2+(b+a*11\pi)^2}$ $F \in [1,2]$, which is related to the plant of the spiral-plate heat exchanger; ρ_c and ρ_h are the densities of the cold fluid and the heat fluid, respectively; c_c and c_h are the specific heat capacities of the cold fluid and the heat fluid, respectively; $T_{c,in}$ and $T_{h,in}$ are the input temperatures of the cold fluid and the heat fluid, respectively; $T_{c,out}$ and $T_{h,out}$ are the output temperatures of the cold fluid and the heat fluid, respectively; q_1 and q_2 are fractional orders of the hot fluid and the cold fluid, respectively; and Q_{L1} and Q_{L2} are the volume flow rate of the hot fluid and the cold fluid, respectively.

$$T_{c,out}(t) = T_{h,in}(t) + FZAD_{11\pi}^{-q}[\frac{1}{k_c Q L_2} + \frac{1}{k_h Q L_1}\Delta T(\theta,t)] + \Delta D_q \tag{4.6}$$

where $T_{c,out}(t) = T(11\pi,t)$, $T_{c,in}(t) = T_h(0,t)$, $T_{h,in}(t) = T_h(11\pi,t)$, $T_{h,out}(t)$ $= T_h(0,t)$. $T_{c,in} - T_{h,out}$ is the initial condition of the fractional order integral.

4.3 Fractional Order Operator Controller Design and Tracking Controller Design

4.3.1 Operator-Based Fractional Order Controller Design

As shown in Figure 2.4, provided a nonlinear operator control system, operators V and Y are the input and output space of this plant. Let (N, D) be the right factorization of P. The feedback nonlinear control system shown in Figure 2.4 is BIBO stable if there exist two stable operators R: Y $\rightarrow$ V, S: V $\rightarrow$ V (S being invertible as well) that satisfy the Bezout identity equation:

$$RN + SD = M \tag{4.7}$$

where M is a unimodular operator to consider the uncertain term in the nonlinear system. With the designed operators S and R in Figure 2.4, the following equation can be satisfied:

$$\|R(N+\Delta N)-RN+S(D+\Delta D)-SD\|<\frac{1}{\|M^{-1}\|} \tag{4.8}$$

where $\|\bullet\|$ is a Lipschitz norm. Then, the nonlinear feedback control system is robustly stable where M is an unimodular operator. The mathematical modeling of P considering the uncertain term ΔP can be provided for the the spiral heat exchanger system as follows:

$P+\Delta P:$

$$T_{c,out}(t)=T_{h,in}(t)+FZ(k+\Delta k)D_{11\pi}^{-q}(\frac{1}{QL_2k_c}+\frac{1}{QL_1k_h})\Delta T(\theta,t))+\Delta D_q \tag{4.9}$$

where $T_{c,out}(t)=T(11\pi,t)$, $T_{c,in}(t)=T_h(0,t)$, $T_{h,in}(t)=T_h(11\pi,t)$, $T_{h,out}(t)$ $=T_h(0,t)$. The plant can be right coprime factorized as follows:

$(D+\Delta D)^{-1}:V\rightarrow W$

$$w=(A+\Delta A)\frac{1}{QL_2k_c}+\frac{1}{QL_1k_h} \tag{4.10}$$

$(D+\Delta D):W\rightarrow V$

$$QL_1=\frac{(A+\Delta A)QL_2k_c}{[QL_2k_cw-(A+\Delta A)]k_h} \tag{4.11}$$

$D:W\rightarrow V$

$$QL_1=\frac{AQL_2k_c}{(QL_2k_cw-A)k_h} \tag{4.12}$$

$N+\Delta N:W\rightarrow Y$

$$T_{c,out}(t)=T_{h,in}(t)+FZ(k+\Delta k)D_{11\pi}^{-q}(w\Delta T(\theta,t))+\Delta D_q \tag{4.13}$$

$N : W \to Y$

$$T_{c,out}(t) = T_{h,in}(t) + FZkD_{11\pi}^{-q}(w\Delta T(\theta, t)) \tag{4.14}$$

The operator-based feedback control system is shown in Figure 2.2. The operators R and S are designed as follows:

$R : Y \to V$

$$b = k_p \frac{1}{FZk} D_{11\pi}^{q}(\Delta T(\theta, t)) \tag{4.15}$$

where $\Delta T(\theta, t) = T_{c,out}(t) - T_{h,in}(t)$.

$S^{-1} : V \to V$

$$Q_{L1} = (K_M - K_p)\frac{AQL_2k_c}{(Q_{L2}k_ce - A)K_h} \tag{4.16}$$

$S : V \to V$

$$e = A(\frac{1}{Q_{L2}k_c} + \frac{1}{Q_{L1}k_h}) \tag{4.17}$$

Operators R and S^{-1} are designed to satisfy the Bezout identity:

$$RN + SD = M \tag{4.18}$$

thus, if

$$\|(R(N + \Delta N) - RN + S(D + \Delta D) - SD))\| < 1/\|M^{-1}\| \tag{4.19}$$

is satisfied according to Therom 5, then the system is BIBO stable.

4.3.2 Fractional Order Operator-Based Control Stability Analysis

In this section, the stability of the fractional order operator-based control system for a spiral-plate exchanger with uncertainties is presented.

$$\begin{aligned} R(N+\Delta N)-RN &= \frac{1}{FZk}D^{q}_{11\pi}(\Delta T)FZ(k+\Delta k)D^{-q}_{11\pi}(w\Delta T)-\frac{1}{FZk}D^{q}_{11\pi}(\Delta T)FZkD^{-q}_{11\pi}(w\Delta T) \\ &= \frac{k+\Delta k}{k}-1 \\ &= \frac{\Delta k}{k} \end{aligned} \tag{4.20}$$

$$\begin{aligned} S(D+\Delta D)-SD &= A\{\frac{[QL_2k_c-(A+\Delta A)]k_h}{k_h(A+\Delta A)QL_2k_c}+\frac{1}{QL_2k_c}\}-A\{\frac{[QL_2k_c-A]k_h}{k_hAQL_2k_c}+\frac{1}{QL_2k_c}\} \\ &= A\{\frac{QL_2k_c-(A+\Delta A)}{(A+\Delta A)QL_2k_c}+\frac{1}{QL_2k_c}\}-A\{\frac{QL_2k_c-A}{AQL_2k_c}+\frac{1}{QL_2k_c}\} \\ &= A\{\frac{1}{A+\Delta A}-\frac{1}{QL_2k_c}+\frac{1}{QL_2k_c}\}-A\{\frac{1}{A}-\frac{1}{QL_2k_c}+\frac{1}{QL_2k_c}\} \\ &= \frac{A}{A+\Delta A}-1 \\ &= -\frac{\Delta A}{A+\Delta A} \end{aligned} \tag{4.21}$$

thus,

$$\begin{aligned} \|R(N+\Delta N)-RN+S(D+\Delta D)-SD\| &= \|\frac{\Delta k}{k}-\frac{\Delta A}{A+\Delta A}\| \\ &< \|\frac{\Delta k}{k}\|+\|\frac{\Delta A}{A+\Delta A}\| \end{aligned} \tag{4.22}$$

According to the stability conditions of the fractional order operator-based control system, if

$$\|\frac{\Delta k}{k}\|+\|\frac{\Delta A}{A+\Delta A}\|<1/\|M^{-1}\| \tag{4.23}$$

that is,

$$\|M^{-1}\|<\frac{1}{\|\frac{\Delta k}{k}\|+\|\frac{\Delta A}{A+\Delta A}\|} \tag{4.24}$$

Here, $k_M = \dfrac{1}{\|M^{-1}\|}$
thus,

$$k_M > \|\frac{\Delta k}{k}\| + \|\frac{\Delta A}{A + \Delta A}\| \tag{4.25}$$

is a BIBO stable condition.

From Table A.1, $\dfrac{\Delta k}{k} = \dfrac{732}{9278} = 0.07$. $\dfrac{\Delta A}{A + \Delta A} = \dfrac{0.135}{0.215} = 0.627$. Let, $k_M > 0.627$, then, the nonlinear control system is BIBO stable.

The fractional order operator-based control system is stable under condition (46), however, the track precision is bad because of model error and disturbances. Therefore, it is rarely used alone. In order to improve the robustness, anti-interference, and tracking performance of the control system, we designed a feedback control system for the tracking controller.

4.3.3 Tracking Controller Design

The differential equation of fractional order controller $PI^{\lambda}D^{\delta}$ is described by

$$u(t) = K_{p1}e(t) + K_i D_t^{-\lambda} e(t) + K_d D_t^{\delta} e(t) \tag{4.26}$$

If $\lambda, \delta = 1$, it is a conventional PID control. It is obvious that the fractional order controller needs to design the three parameters K_{p1}, K_i, and K_d as well as the orders λ, δ of the integral and derivative controllers. The orders λ, δ need not necessarily be integers, and can be any real numbers. As shown in Figure 4.1, the FOPID (fractional order PID) controller generalizes the conventional integer order PID controller and expands it from point to plane. This expansion can provide a great deal more flexibility in PID control design.

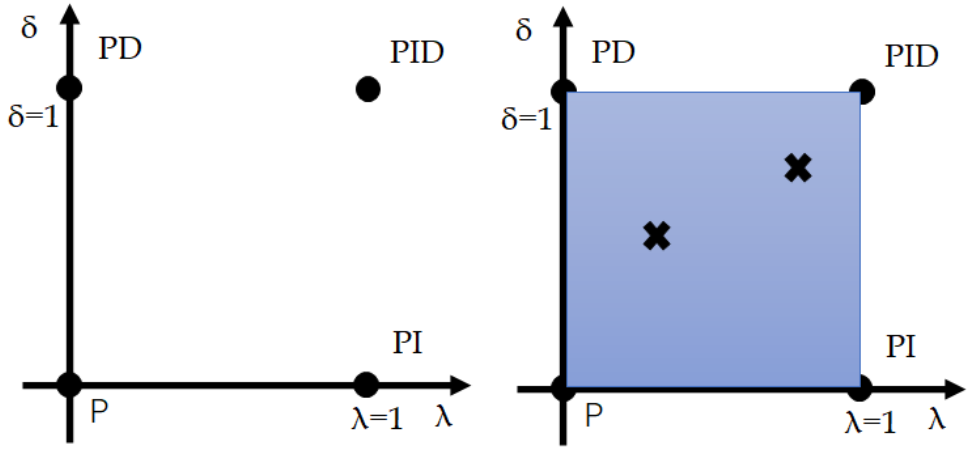

Figure 4.1: FOPID controller

4.3.4 Operator-Based Fractional Order Robust Control for Spiral-Plate Heat Exchanger with Uncertainties and Disturbances

As a spiral heat exchanger is a nonlinear system with uncertainties, disturbances, and a long delay time, it is difficult to improve the tracking performance of the output temperature. While operator-based control is a nonlinear control method to improve stability, tracking performance remains poor. PID feedback control is widely used in application due to its simple form and because it only required three parameters to be adjusted. FOPID, with its five parameters, is an extension of conventional PID. Thus, FOPID is more flexible than the conventional PID. The five cases for output temperature control of the presented spiral heat exchanger were designed to compare tracking performance and stablity for uncertanities and disturbance, as shown Figures 4.2–4.6.

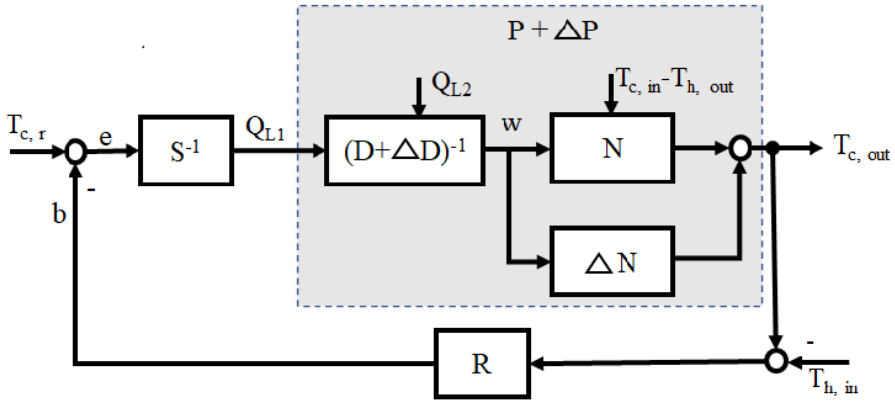

Figure 4.2: Operator-based fractional order robust control.

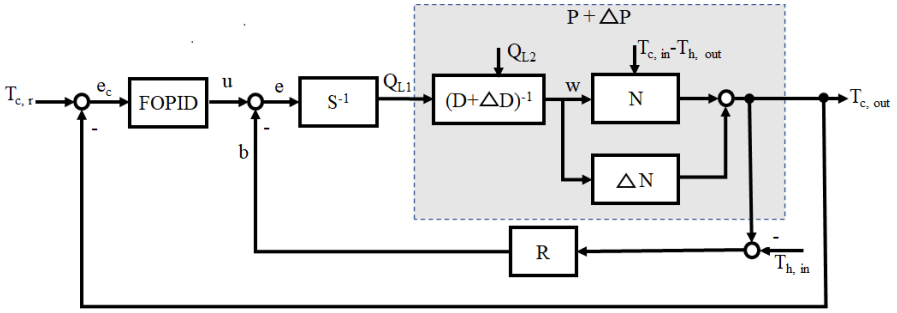

Figure 4.3: Operator-based fractional order robust control with FOPID controller.

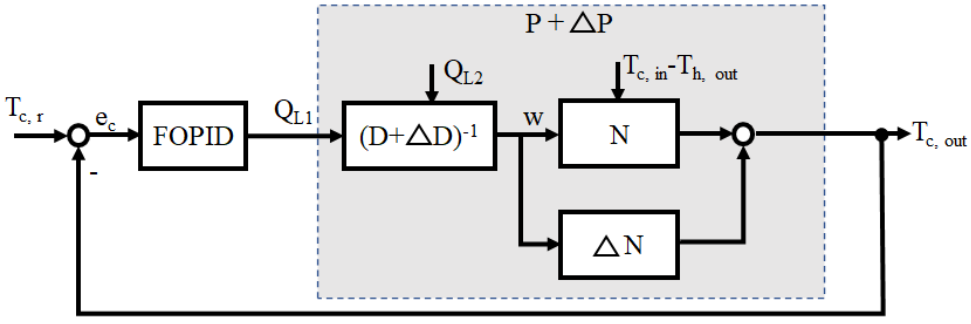

Figure 4.4: Fractional order robust control with FOPID controller.

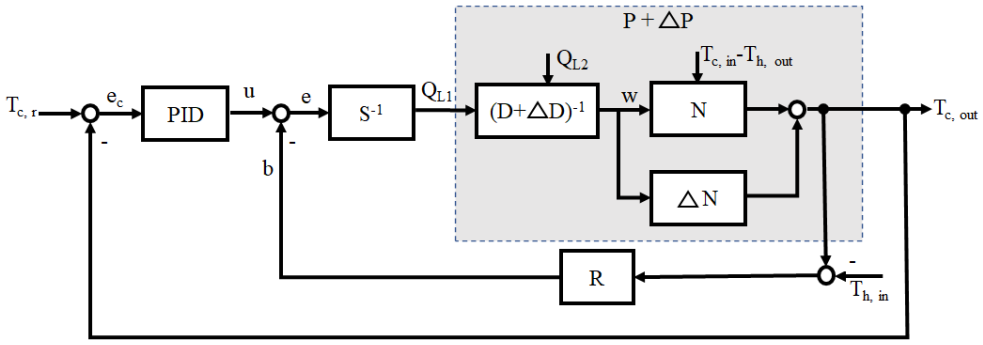

Figure 4.5: Operator-based fractional order robust control with PID controller.

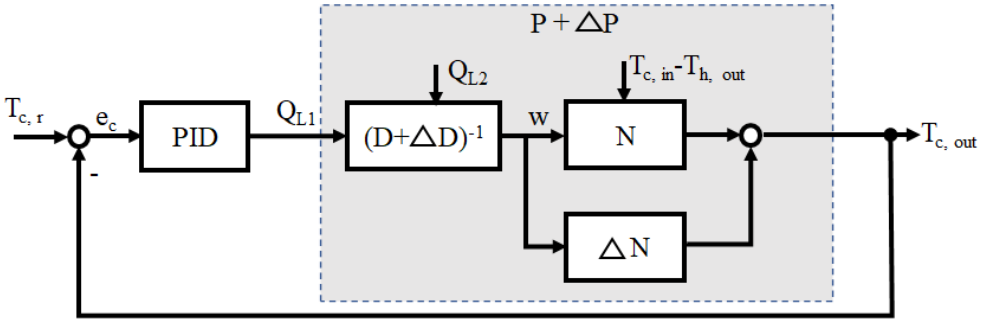

Figure 4.6: Fractional order robust control with PID controller.

4.4 Simulations and Analysis

In this section, the five different cases are simulated and analysed in Matlab with the same uncertainties and disturbances.

4.4.1 Simulation Conditions

Here, Table 4.1 shows the simulation parameters for the spiral-plate heat exchanger. Table 4.2 denotes the simulation condition for the spiral-plate heat exchanger. The reference output temperature is the output temperature

of the cold fluid. The volume flow rate QL_2 on the cold fluid side is the disturbance signal; QL_2 is changed from 1 L/Min to 7 L/Min in time 8s, $\frac{\Delta A}{A}$ and $\frac{\Delta k}{k}$ are the uncertainties of the spiral heat exchanger's shape and the heat transfer coefficient, respectively. The volume flow rate QL_1 on the hot fluid side is the control signal. Considering the actual condition, the maximum input volume flow rate is 10 L/Min.

Table 4.1: Simulation parameters of the spiral-plate heat exchanger.

Meaning (Symbol)	**Value**
The densities of the two fluids (ρ_c, ρ_h)	1000 Kg/m^3
The specific heat capacities of two fluids (c_c, c_h)	4.2 KJ/(Kg·°C)
The input temperature of cold fluid ($T_{c,in}$)	20 °C
The input temperature of hot fluid ($T_{h,in}$)	50 °C
Thermal conductivity of SUS304 (λ)	16.7 W/(m °C)
Heat transfer coefficients of two fluids (h_h, h_c)	366 W/m^2· K
Uncertainty of the spiral heat exchanger's shape (ΔA)	0.135
Uncertainty of the heat transfer coefficient (Δk)	732

Table 4.2: Simulation condition of the spiral-plate heat exchanger.

Meaning (Symbol)	**Value**
Simulation time(t)	[0, 15] s
Reference output temperature ($T_{c,r}$)	40 °C
The orders for fractional order derivative (q)	0.97
The input temperature of cold fluid ($T_{c,in}$)	20 °C
The input temperature of hot fluid ($T_{h,in}$)	50 °C
Uncertainty of the spiral heat exchanger's shape ($\frac{\Delta A}{A}$)	0.627
Uncertainty of the heat transfer coefficient ($\frac{\Delta k}{k}$)	0.07

4.4.2 Simulations and Analysis

The spiral counter-flow heat exchanger with uncertainties and disturbances described by the special fractional order equation is both a first order or norm

fractional order system and a nonlinear system. Thus, the parameters of fractional order PID control cannot be tuned using the conventional tuning method. The parameters of both the conventional and fractional order PID control are tuned using a trial-and-error method. The first proportion is adjusted, then derivative integrals are adjusted in turn until the best parameters are derived. Tables 4.3–4.7 are the best controller parameters to tune and the parameters of the operator controller.

Table 4.3: Tuning parameters for operator controller.

Meaning	**Symbol**	**Value**
Reference input temperature	$T_{c,r}$	40 °C
The orders for fractional order derivative (q)	0.97	
Gain of operator	K_{p1}	10
Gain	K_M	4.0

Table 4.4: Tunning parameters for FOPID Controller with operator controller.

Meaning	**Symbol**	**Value**
Reference input temperature	$T_{c,r}$	40 °C
The orders for fractional order derivative (q)	0.97	
Gain of operator	K_{p1}	10
Gain	K_M	4.0
Proportional gain	K_{p1}	50
Integeral order	λ	0.9
Integeral gain	K_i	1.0
Differential order	δ	0.95
Differential gain	K_d	3.0

Table 4.5: Tunning parameters for FOPID Controller without operator controller.

Meaning	**Symbol**	**Value**
Reference input temperature	$T_{c,r}$	40 °C
Proportional gain	K_{p1}	50
Integeral order	λ	0.9
Integeral gain	K_i	1.0
Differential order	δ	0.95
Differential gain	K_d	3.0

Table 4.6: Tunning parameters for PID Controller with operator controller.

Meaning	**Symbol**	**Value**
Reference input temperature	$T_{c,r}$	40 °C
The orders for fractional order derivative (q)	0.97	
Gain of operator	K_{p1}	10
Gain	K_M	4.0
Proportional gain	K_{p1}	10
Integeral gain	K_i	0.6
Differential gain	K_d	0.05

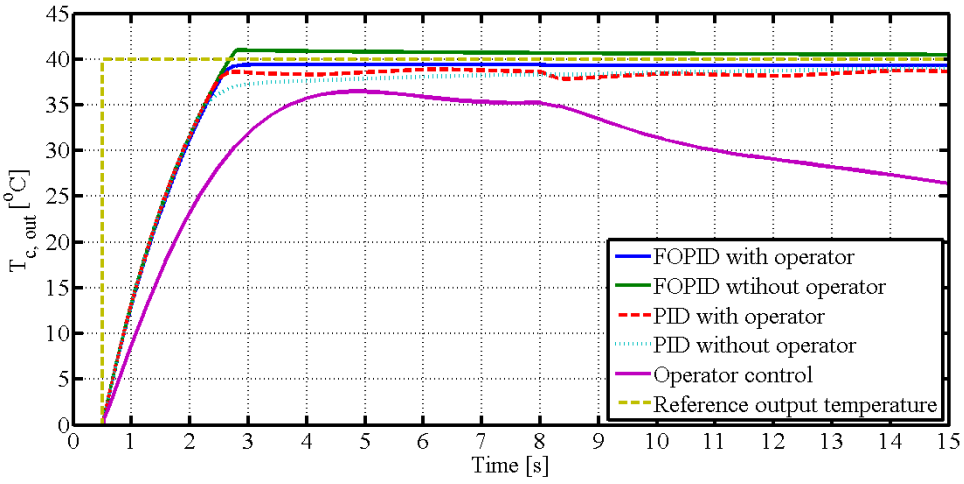

Figure 4.7: Comparison of different control schemes.

Table 4.7: Tunning parameters for PID Controller without operator controller.

Meaning	**Symbol**	**Value**
Reference input temperature	$T_{c,r}$	40 °C
The orders for fractional order derivative (q)	0.97	
Proportional gain	K_{p1}	10
Integeral gain	K_i	0.6
Differential gain	K_d	0.05

It is obvious that the fractional order PID control with operator controller has the best tracking performance compared to the others, as shown in Figure 4.7. The overshoot and settle times for the fractional order PID control with operator controller are shorter than for the fractional order PID control without operator controller. The overshoot and settle times for the conventional PID control with operator controller are smaller than for the conventional PID control without operator controller.

Figure 4.8 shows that fractional order operator control can improve the stability when uncertainties and disturbances are present, although the tracking performance and anti-disturbance are bad. Figures 4.9–4.12 show the control performance, control signals, and tracking performance in the control process for the five different control schemes with uncertainties and disturbances; $T_{c,\ r}$, d, u, and $T_{c,\ out}$ are the reference output temperature of the cold fluid side, disturbance signal of the volume flow rate in the cold fluid side, control signal of the volume flow rate on the hot fluid side, and output temperature on the cold fluid side, respectively. The performance with operator-based fractional order PID control is the best in terms of anti-disturbance and stability compared to the other control schemes.

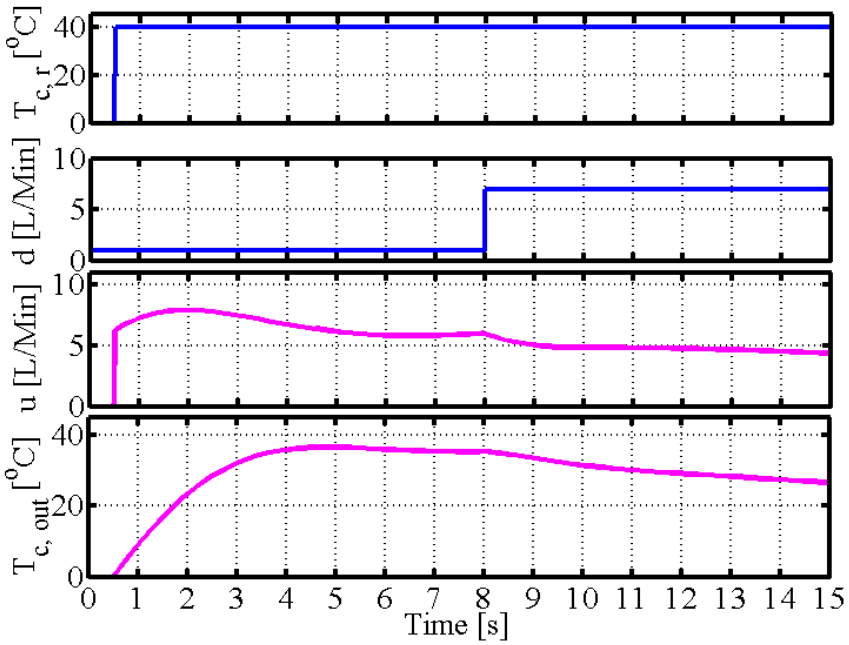

Figure 4.8: Simulation of operator control.

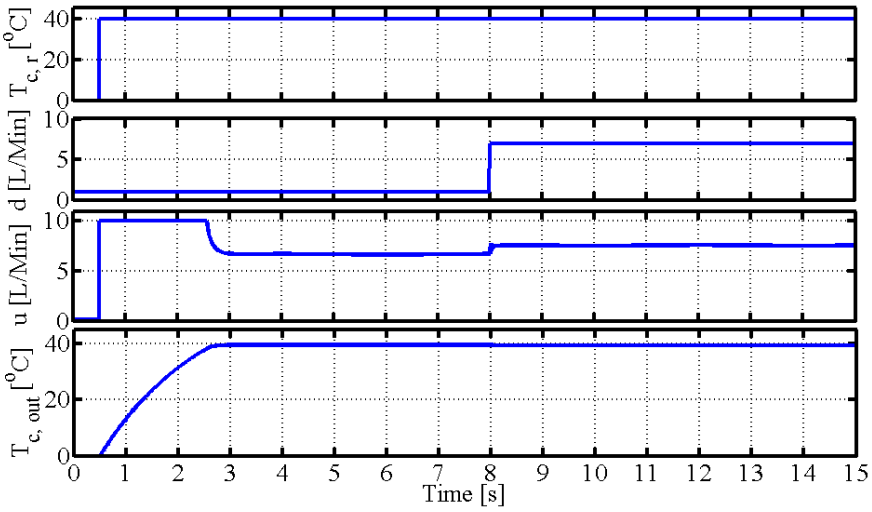

Figure 4.9: Simulation of FOPID with operator.

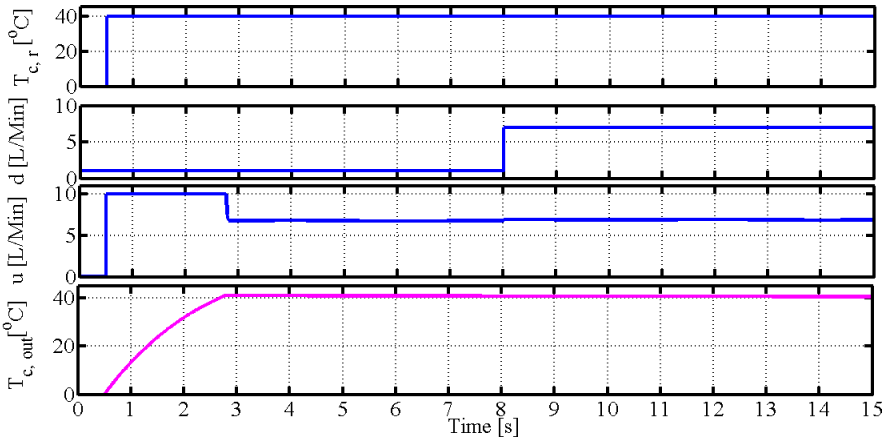

Figure 4.10: Simulation of FOPID without operator.

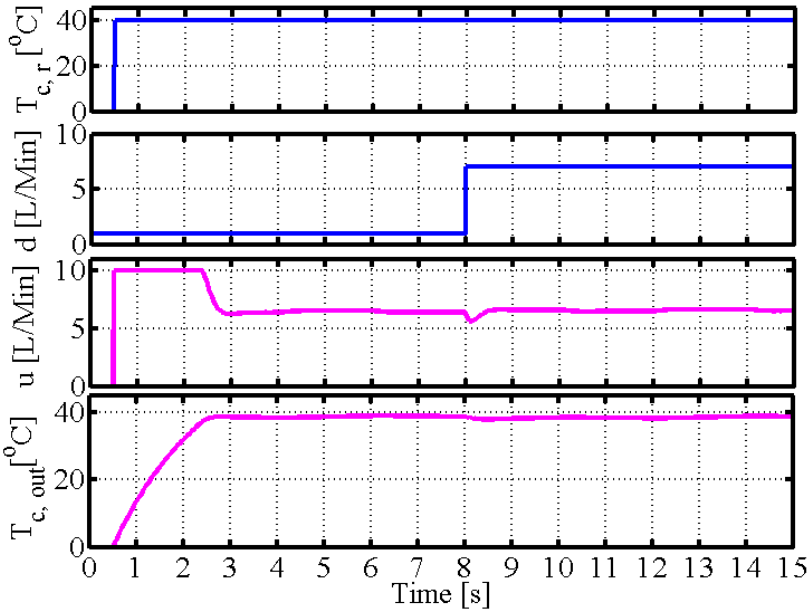

Figure 4.11: Simulation of PID with operator.

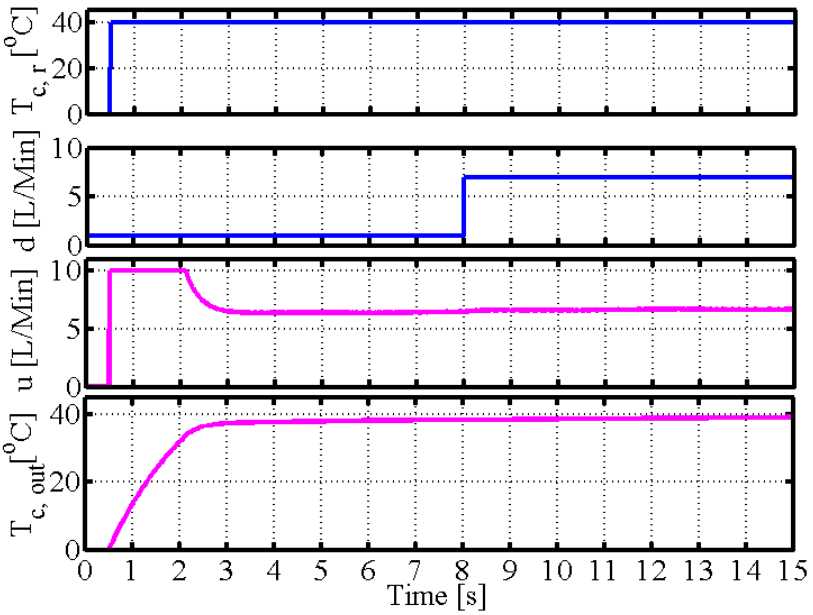

Figure 4.12: Simulation of PID without operator.

4.5 Conclusion

In this dissertation, we have proposed operator-based fractional order nonlinear robust control with uncertainties and disturbance. First, we introduced the concepts of fractional order and the preliminaries of operator theory as extended to fractional order and nonlinear fractional order equations. Then, operator-based nonlinear fractional order controller design and fractional order PID tracking controller design were covered and the parameters of the operator controller and fractional order PID controller were determined. Finally, the robust stability and tracking performance of the operator-based nonlinear robust control system with uncertainties and disturbance were analyzed via simulation in Matlab. However, the tuning parameters of the fractional order controller continue to require adjustment offline or by hand, and robust control performance requires continued research as well.

Chapter 5

Operator-Based Fractional-Order Nonlinear Robust Control for the Spiral Heat Exchanger Identified by Particle Swarm Optimization

5.1 Introduction

In this chapter, an operator-based fractional-order nonlinear robust control for the spiral heat exchanger described by a parallel fractional-order model is proposed. The parallel fractional-order model for the spiral heat exchanger is identified by PSO and the parameters of FOPID controller are optimized by PSO.

In Section 5.2, problem statement is presented.

In Section 5.3, the parallel fractional-order model for the spiral counter-flow heat exchanger is introduced. The parallel fractional-order model for the spiral counter-flow heat exchanger is identified by PSO, with the least squares method as the performance index.

In Section 5.4, an operator-based fractional-order nonlinear robust control

for the spiral heat exchanger described by the identified parallel fractional-order model is proposed. Then, the parallel fractional-order operator controller is designed.

In Section 5.5, the parameters of the fractional-order PID controller are optimized by PSO.

In Section 5.6, comparisons of two control schemes are performed to analyze the tracking and antidisturbance performance for the spiral counter-flow heat exchanger, and the effectiveness is verified.

5.2 Statement Problem

A spiral heat exchanger is a nonlinear system with uncertainties. It is used widely in industry. In real application, the heated or cooled output temperature should track a timely reference input temperature in variable load conditions. However, the output temperature of the spiral heat exchanger is difficult to control for nonlinearity, uncertainties, and many disturbances. In conventional control methods, a PID controller is used to derive a good control performance in slow or no disturbances. In real application, there are many disturbances for the spiral heat exchanger, such as input temperature and flow rate on the hot-fluid side, input temperature on the cold-fluid side. Thus, due to the disturbances, control performance is poor in conventional control methods.

5.3 Fractional-Order System Identification for the Spiral Heat Exchanger by PSO

5.3.1 Parallel Fractional-Order Model for the Spiral Counter-Flow Heat Exchanger

Fractional-Order Model for the Spiral Counter-Flow Heat Exchanger

According to the law of heat energy balance of two fluids, the fractional-order derivative model for the spiral-plate counter-flow heat exchanger is derived as follows [45].

$$\begin{cases} D_\theta^{q_1} T_h(\theta,t) = \dfrac{(k+\Delta k)FAZ}{QL_1 c_h \rho_h}(T_c(\theta,t) - T_h(\theta,t) \\ D_\theta^{q_2} T_c(\theta,t) = \dfrac{(k+\Delta k)FAZ}{QL_2 c_c \rho_c}(T_h(\theta,t) - T_c(\theta,t) \\ \theta \in [0, 11\pi] \end{cases} \tag{5.1}$$

where $k = \frac{\delta_s}{\lambda}$, $k + \Delta k = \frac{1}{h_h} + \frac{\delta_s}{\lambda} + \frac{1}{h_c}$, $k_c = c_c\rho_c$, $k_h = c_h\rho_h$, and $\Delta T(\theta,t)$ $= T_c(\theta,t) - T_h(\theta,t)$. $A = \sqrt{a^2+b^2}$, and $A + \Delta A = \sqrt{a^2 + (b + a * 11\pi)^2}$ $F \in [1,2]$, which is related to the plant of the spiral-plate heat exchanger. ρ_c, ρ_h are the densities of the cold fluid and the hot fluid, respectively. c_c, c_h are the specific heat capacities of the cold fluid and the hot fluid, respectively.

Parallel Fractional-Order Model for the Spiral Counter-Flow Heat Exchanger

The parallel fractional-order model for the spiral-plate counter-flow heat exchanger is described as follows.

$$\begin{cases} T_{hk} = (\Delta\theta)^{q_1} D_{hfrac} + B_h T_{hk-1} \\ T_{ck} = (\Delta\theta)^{q_2} D_{cfrac} + B_c T_{ck-1} \end{cases} \tag{5.2}$$

where $T_{hk}, T_{hk-1}, D_{hfrac} \in R^N$, $B_h \in R^{N\times N}$, $T_{ck}, T_{ck-1}, D_{cfrac} \in R^N$, and $B_c \in R^{N\times N}$

$$T_{hk} = \begin{pmatrix} T_h(\Delta\theta) \\ T_h(2(\Delta\theta)) \\ \vdots \\ T_h(N(\Delta\theta)) \end{pmatrix} \tag{5.3}$$

$$B_h = \begin{pmatrix} \frac{-\Gamma(q_1+1)}{\Gamma(2)\Gamma(q_1)} & 0 & \cdots & 0 \\ \frac{\Gamma(q_1+1)}{\Gamma(3)\Gamma(q_1-1)} & \frac{-\Gamma(q_1+1)}{\Gamma(2)\Gamma(q_1)} & \cdots & 0 \\ \vdots & \vdots & \vdots & \vdots \\ \frac{(-1)^N\Gamma(q_1+1)}{\Gamma(N+1)\Gamma(q_1-N+1)} & \frac{(-1)^{(N-1)}\Gamma(q_1+1)}{\Gamma(N)\Gamma((q_1-N+1)} & \cdots & \frac{-\Gamma(q_1+1)}{\Gamma(2)\Gamma(q_1)} \end{pmatrix} \tag{5.4}$$

$$T_{hk-1} = \begin{pmatrix} T_h(0) \\ T_h(\Delta\theta) \\ \vdots \\ T_h((N-1)(\Delta\theta)) \end{pmatrix} \tag{5.5}$$

$$B_c = \begin{pmatrix} \frac{-\Gamma(q_2+1)}{\Gamma(2)\Gamma(q_2)} & 0 & \cdots & 0 \\ \frac{\Gamma(q_2+1)}{\Gamma(3)\Gamma(q_2-1)} & \frac{-\Gamma(q_2+1)}{\Gamma(2)\Gamma(q_2)} & \cdots & 0 \\ \vdots & \vdots & \vdots & \vdots \\ \frac{(-1)^N\Gamma(q_2+1)}{\Gamma(N+1)\Gamma(q_2-N+1)} & \frac{(-1)^{(N-1)}\Gamma(q_2+1)}{\Gamma(N)\Gamma((q_2-N+1)} & \cdots & \frac{-\Gamma(q_2+1)}{\Gamma(2)\Gamma(q_2)} \end{pmatrix} \tag{5.6}$$

$$T_{ck} = \begin{pmatrix} T_c(\Delta\theta) \\ T_c(2\Delta\theta) \\ \vdots \\ T_c(N(\Delta\theta)) \end{pmatrix} \tag{5.7}$$

$$T_{ck-1} = \begin{pmatrix} T_c(0) \\ T_c(\Delta\theta) \\ \vdots \\ T_c((N-1)(\Delta\theta)) \end{pmatrix} \tag{5.8}$$

Therefore, the parallel fractional-order derivative model for the spiral-plate counter-flow heat exchanger is obtained.

$$\begin{cases} T_{hk} = (\Delta\theta)^{q_1} \dfrac{FkZA}{QL_1 c_h \rho_h}(HT_{cK-1} - T_{hK-1}) + B_h T_{hk-1} \\ T_{ck} = (\Delta\theta)^{q_2} \dfrac{FkZA}{QL_2 c_c \rho_c}(HT_{hK-1} - T_{cK-1}) + B_c T_{ck-1} \\ T_{cout} = CT_{ck} \end{cases} \tag{5.9}$$

where

$$H = \begin{pmatrix} 0 & 0 & 0 & \dots & 0 & 1 \\ 0 & 0 & 0 & \dots & 1 & 0 \\ \vdots & \vdots & \vdots & \vdots & \vdots & \vdots \\ 1 & 0 & 0 & \dots & 0 & 0 \end{pmatrix} \tag{5.10}$$

$$C = \begin{pmatrix} 0 & 0 & 0 & 0 & \dots & 1 \end{pmatrix} \tag{5.11}$$

where $C \in R^{1\times N}$ and $H \in R^{N\times N}$. The parallel fractional-order model for the spiral counter-flow heat exchanger is a model with parallel input data.

5.3.2 Parallel Fractional-Order Model Identification for the Spiral Heat Exchanger

The schematic block of the parameter estimation for a parallel fractional-order model of the spiral counter-flow heat exchanger is shown in Figure 5.1.

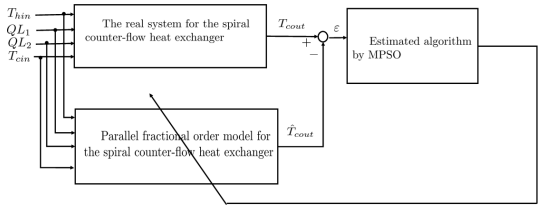

Figure 5.1: The schematic block of parameter estimation for the parallel fractional-order model of the spiral counter-flow heat exchanger.

The specific parameter estimation steps are follows.

(1) Determine the searched spaces for the estimated model.

Let $K_h = \dfrac{FkZA}{c_h\rho_h}$, $K_c = \dfrac{FkZA}{c_c\rho_c}$, then the parallel fractional-order model for the spiral counter-flow heat exchanger derived from (5.9) is the model's identified object as follows.

$$\begin{cases} T_{hk} = (\Delta\theta)^{q_1}\dfrac{K_h}{QL_1}(HT_{cK-1} - T_{hK-1}) + B_hT_{hk-1} \\ T_{ck} = (\Delta\theta)^{q_2}\dfrac{K_c}{QL_2}(HT_{hK-1} - T_{cK-1}) + B_cT_{ck-1} \\ T_{cout} = CT_{ck} \end{cases} \tag{5.12}$$

The researched space vector is defined as

$$x = \{q_1, q_2, K_h, K_c\} \tag{5.13}$$

where K_h, K_c are the model parameters and q_1, q_2 are the orders of the model. The range of the model parameter (K_h, K_c) was set to be [0 10], and the range of the model parameter (q_1, q_2) was set to be [0 2].

(2) Determine the performance index (evaluation function).

In this paper, the input flow rate of the hot-fluid side QL_1, the input flow rate of the cold-fluid side QL_2, the input temperature of the cold-fluid side T_{cin}, and the input temperature of the hot-fluid side T_{hin} were introduced as input signals of identified object. The sum of the squared errors between the output $\hat{T}_{cout}$ and the true value $\hat{T}_{cout}$,

$$J = \int_0^T [T_{cout}(t) - \hat{T}_{cout}(t)]^2 dt \tag{5.14}$$

was used as the performance evaluation function.

(3) The parameters of the algorithm are initialized to generate random search vectors.

(4) According to the steps of the PSO algorithm, the parameters in the parallel fractional-order model are identified.

(5) The iteration is repeated until the performance index is satisfactory or the sum of iterations go up to a maximum of 200.

The evolutionary curves of the estimated parameters are plotted in Figures 5.2–5.5.

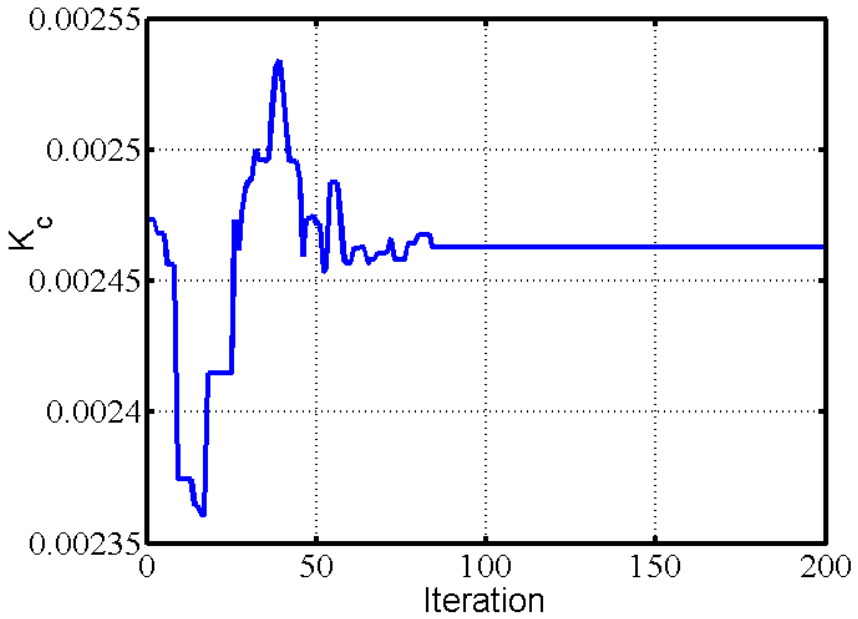

Figure 5.2: Evolutionary curve of the estimation of K_c.

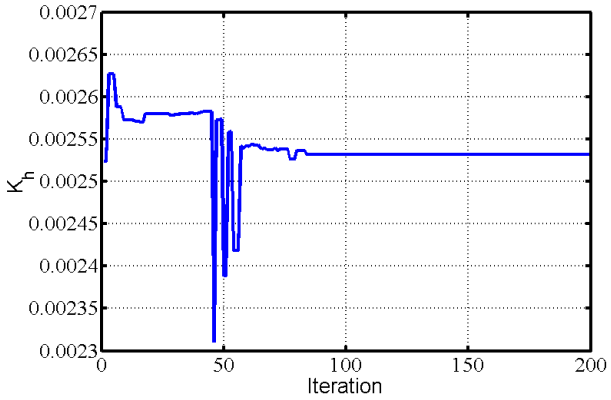

Figure 5.3: Evolutionary curve of the estimation of K_h.

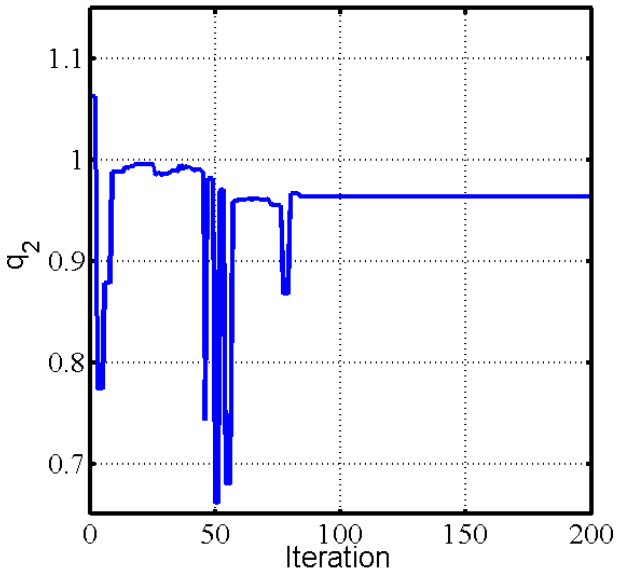

Figure 5.4: Evolutionary curve of the estimation of q_2.

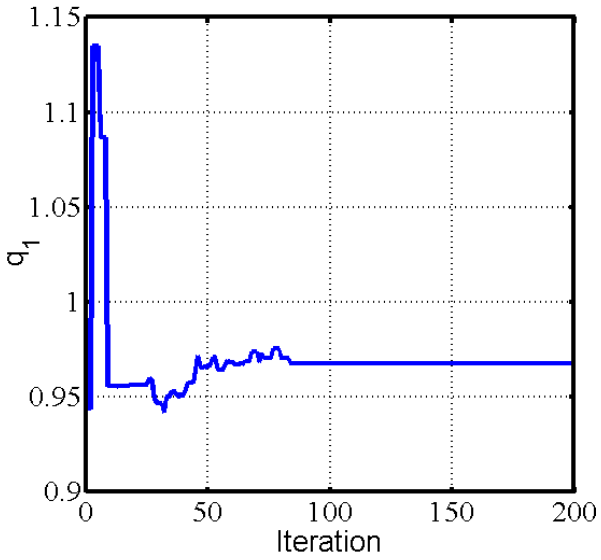

Figure 5.5: Evolutionary curve of the estimation of q_1.

The evolutionary curve of the performance index is plotted in Figure 5.6.

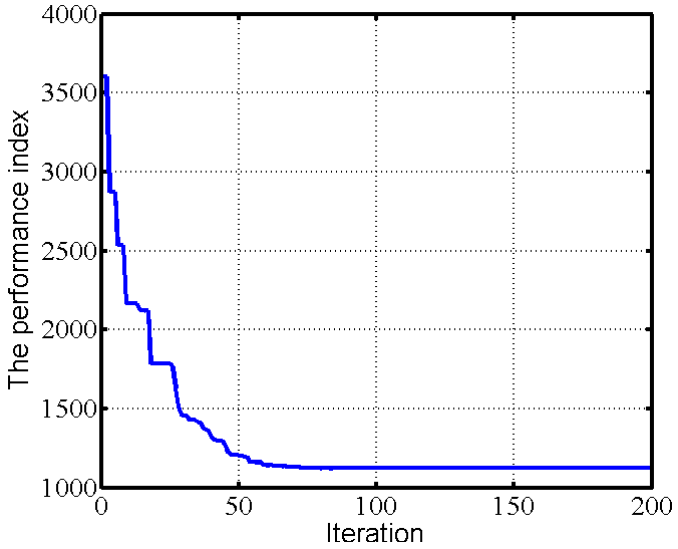

Figure 5.6: Evolutionary curve of the performance index.

The comparison of the output value from the identification system and the true value from the experiment is shown in Figure 5.7.

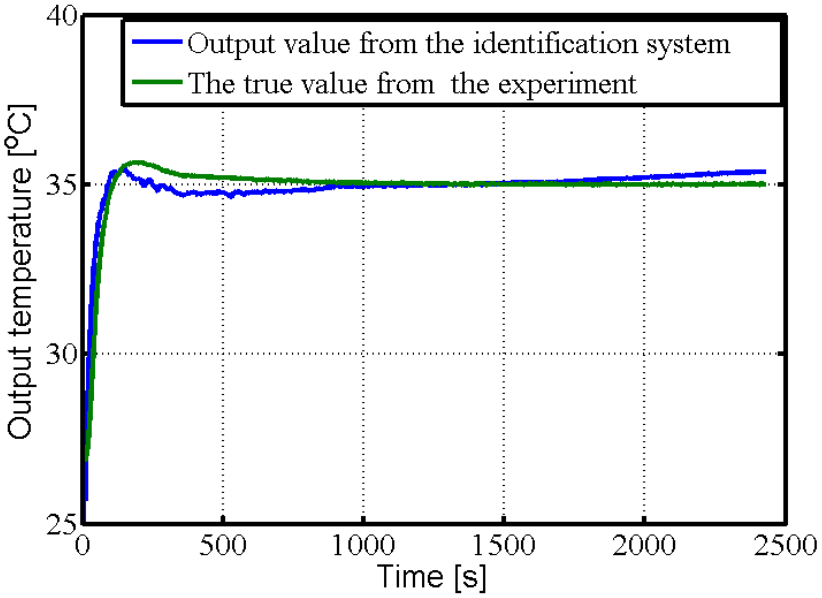

Figure 5.7: Comparison of the output value from the identification system and the true value from the experiment.

5.4 Operator-Based Fractional-Order PID Nonlinear Robust Control for the Spiral Heat Exchanger

In this section, two control schemes were designed in order to verify the tracking and antidisturbance performance of the operator-based fractional-order PID nonlinear robust control of the spiral heat exchanger, as shown Figures 5.8 and 5.9.

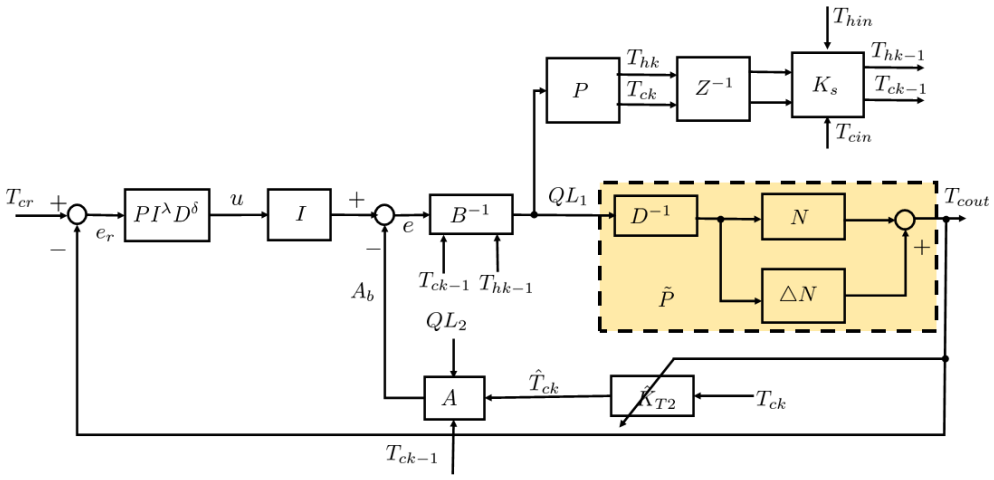

Figure 5.8: FOPID controller with operator.

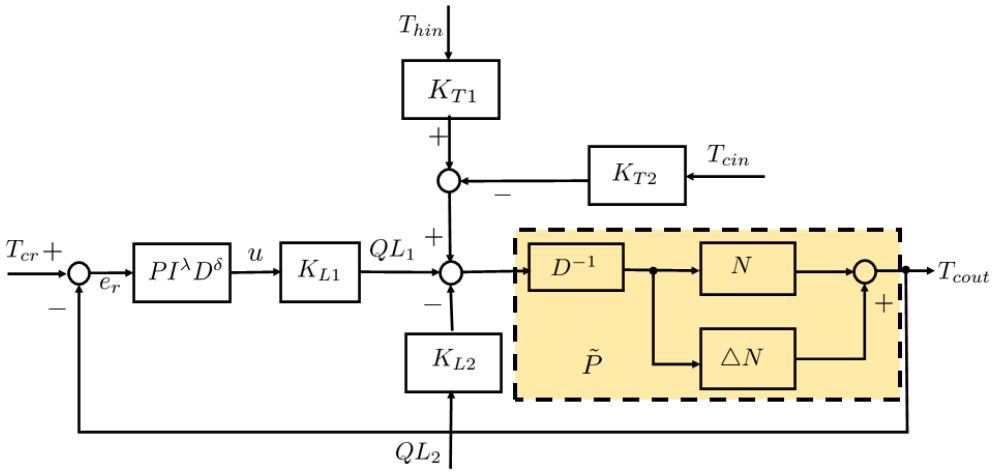

Figure 5.9: FOPID controller without operator.

5.4.1 Parallel Fractional-Order Model for the Spiral Heat Exchanger with Uncertainties

The heat transfer coefficient of the spiral heat exchanger plant $\tilde{k}$ is a relationship between not only the flow velocity of water, but also others. We

know that the spiral heat exchanger model is nonlinear. Therefore, the spiral heat exchanger model is nonlinear system with uncertainties. The nonlinear fractional-order equations for the spiral heat exchanger model are described as follows.

$$\begin{cases} T_{hk} = (\Delta\theta)^{q_1} \dfrac{K_h}{QL_1}(HT_{cK-1} - T_{hK-1}) + B_h T_{hk-1} \\ T_{ck} = (\Delta\theta)^{q_2} \dfrac{K_c}{QL_2}(HT_{hK-1} - T_{cK-1}) + B_c T_{ck-1} \\ T_{cout} = CT_{ck} \end{cases} \tag{5.15}$$

$$\begin{cases} T_{hk} = (\Delta\theta)^{q_1} \dfrac{(k+\Delta k)ZA_1}{QL_1 c_h \rho_h}(HT_{cK-1} - T_{hK-1}) + B_h T_{hk-1} \\ T_{ck} = (\Delta\theta)^{q_2} \dfrac{(k+\Delta k)ZA_2}{QL_2 c_c \rho_c}(HT_{hK-1} - T_{cK-1}) + B_c T_{ck-1} \\ T_{cout} = CT_{ck} \end{cases} \tag{5.16}$$

$$k = \frac{\delta_s}{\lambda} \tag{5.17}$$

where Δk are the uncertainties for the spiral heat exchanger.

5.4.2 Operator-Based Controller Design

In Figure 5.10, we show an operator nonlinear control system, where operators V and Y are the input and output spaces of this plant. Let (N, D) be the right factorization of P. The feedback nonlinear control system shown in Figure 5.10 is BIBO stable if there exist two stable operators A: Y $\rightarrow$ V, B: V $\rightarrow$ V (B is also invertible) satisfying Bezout's identity equation.

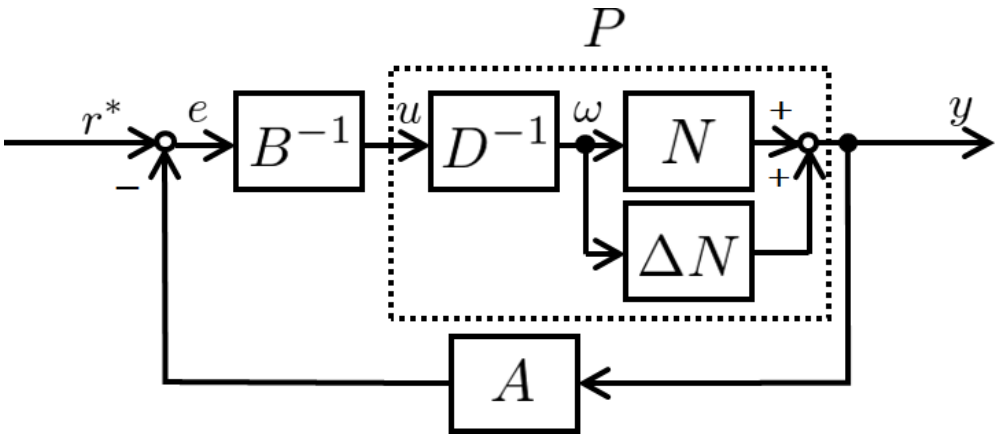

Figure 5.10: Nonlinear feedback control system with uncertainties. The plant P is a nonlinear system with uncertainty ΔN, r^* is the reference input signal.

$$AN + BD = M \tag{5.18}$$

where M is a unimodular operator. Considering the uncertain term in the nonlinear system, with the designed operators A and B in Figure 5.10, the following equation could be satisfied.

$$\|A((N + \Delta N) - AN)M^{-1}\|_{Lip} < 1 \tag{5.19}$$

where $\|\bullet\|_{Lip}$ is a Lipschitz norm. Then, the nonlinear feedback control system has robust stability and M is a unimodular operator. The mathematical modeling $\tilde{P}$ considering the uncertain term ΔP can be given for the the spiral heat exchanger system as follows.

P :

$$\begin{cases} T_{hk} = (\Delta\theta)^{q_1} \dfrac{kZA_1}{QL_1c_h\rho_h}(HT_{cK-1} - T_{hK-1}) + B_hT_{hk-1} \\ T_{ck} = (\Delta\theta)^{q_2} \dfrac{kZA_2}{QL_2c_c\rho_c}(HT_{hK-1} - T_{cK-1}) + B_cT_{ck-1} \\ T_{cout} = CT_{ck} \end{cases} \tag{5.20}$$

K_s :

$$T_{hk-1} = \begin{pmatrix} 0 & 0 & \dots & 0 & 0 \\ 1 & 0 & \dots & 0 & 0 \\ 0 & 1 & \dots & 0 & 0 \\ \vdots & \vdots & \vdots & \vdots & \vdots \\ 0 & 0 & \dots & 1 & 0 \end{pmatrix} T_{hk} + \begin{pmatrix} 1 \\ 0 \\ 0 \\ \vdots \\ 0 \end{pmatrix} T_{hin} \tag{5.21}$$

$$T_{ck-1} = \begin{pmatrix} 0 & 0 & \dots & 0 & 0 \\ 1 & 0 & \dots & 0 & 0 \\ 0 & 1 & \dots & 0 & 0 \\ \vdots & \vdots & \vdots & \vdots & \vdots \\ 0 & 0 & \dots & 1 & 0 \end{pmatrix} T_{ck} + \begin{pmatrix} 1 \\ 0 \\ 0 \\ \vdots \\ 0 \end{pmatrix} T_{cin} \tag{5.22}$$

where Z^{-1} denotes a time delay of one sample period.

$P + \Delta P$:

$$\begin{cases} T_{hk} = (\Delta\theta)^{q_1} \dfrac{(k+\Delta k)ZA_1}{QL_1c_h\rho_h}(HT_{cK-1} - T_{hK-1}) + B_hT_{hk-1} \\ T_{ck} = (\Delta\theta)^{q_2} \dfrac{(k+\Delta k)ZA_2}{QL_2c_c\rho_c}(HT_{hK-1} - IT_{cK-1}) + B_cT_{ck-1} \\ T_{cout} = CT_{ck} \end{cases} \tag{5.23}$$

The plant can be right-coprime-factorized as follows.

$N + \Delta N : W \to Y$

$$T_{ck} = (\Delta\theta)^{q_2} \frac{(k+\Delta k)ZA_2}{QL_2c_c\rho_c}(Hw - T_{cK-1}) + B_cT_{ck-1} \tag{5.24}$$

$D^{-1} : V \to W$

$$w = (\Delta\theta)^{q_1}(\frac{kA_1Z}{QL_1c_h\rho_h\delta_h}(HT_{cK-1} - T_{hK-1})) + B_hT_{hk-1} \tag{5.25}$$

The operator-based feedback control system is shown in Figure 5.8. The operators A and B were designed as follows.

$A : Y \to V$

$$b = (1 - K_p)H^{-1}[T_{ck-1} + \frac{QL_2c_c\rho_c}{(\Delta\theta)^{q_2}ZkA_2}(\hat{T}_{ck} - B_cT_{ck-1})] \tag{5.26}$$

$$\hat{T}_{ck} = \frac{T_{cout}}{T_{ck}(end)}T_{ck} \tag{5.27}$$

$B^{-1} : V \to V$

$$QL_1 = (\Delta\theta)^{q_1}k_p\frac{ZkA_1(HT_{cK-1} - T_{hK-1})}{c_h\rho_h(e - B_hT_{hk-1})} \tag{5.28}$$

Operators A and B^{-1} were designed to satisfy the Bezout identity and k_p is the gain to be determined.

$$\|A((N + \Delta N) - AN)M^{-1}\|_{Lip} < 1 \tag{5.29}$$

5.4.3 Fractional-Order Tracking Controller Design

The differential equation of fractional-order controller $PI^{\lambda}D^{\delta}$ is described as follows.

$$q(t) = K_{p1}e(t) + K_iD_t^{-\lambda}e(t) + K_dD_t^{\delta}e(t) \tag{5.30}$$

It is obvious that the fractional-order controller not only need three parameters K_{p1}, K_i, and K_d, but also two orders λ, δ of integral and derivative controller. The orders λ, δ are not necessarily integers, but any real numbers. As shown in Figure 5.11, the FOPID (fractional-order PID) controller generalizes the conventional integer-order PID controller and expands it from a point to a plane. This expansion could provide much more flexibility in PID controller design.

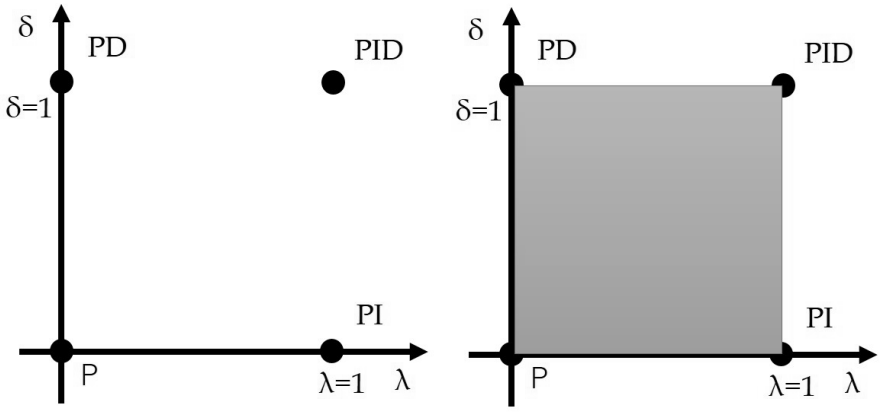

Figure 5.11: PID controller with the fractional orders.

5.5 Parameter Optima for Fractional-Order PID Controller

The specific parameter estimation steps were follows.

(1) Determine the searched spaces for the fractional-order PID controller.

The researched space vector was defined as

$$x = \{K_p, K_i, K_d, \lambda, \mu\} \tag{5.31}$$

where K_p, K_i, K_d are the gains and λ, μ are the orders. The range of the model parameter (K_p, K_i, K_d) was set to be [0 100], and the range of the model parameter (λ, μ) was set to be [0 1].

(2) Determine the performance index (evaluation function).

For determining the optimum values of the gains of the controller, the integral of time multiplied by the absolute value of the error (ITAE), the

integral of the absolute value of the error (IAE), the integral of time multiplied by the squared error (ITSE), and the integral of the squared error (ISE) were taken as objective functions. The expression for these error functions are given below:

$$ITAE = \int_0^T t|T_{cr}(t) - T_{cout}(t)|dt \tag{5.32}$$

$$IAE = \int_0^T |T_{cr}(t) - T_{cout}(t)|dt \tag{5.33}$$

$$ITSE = \int_0^T t(T_{cr}(t) - T_{cout}(t))^2 dt \tag{5.34}$$

$$ISE = \int_0^T (T_{cr}(t) - T_{cout}(t))^2 dt \tag{5.35}$$

where T_{cout} is the output temperature, T_{cr} is the reference input temperature, and T is the time range of the simulation. In this paper, The ITSE was used as the performance evaluation function.

(3) The parameters of the algorithm are initialized to generate random search vectors.

(4) According to the steps of the PSO algorithm, the parameters of fractional-order PID controller are identified.

(5) The iteration is repeated until the performance index is satisfactory or the sum of iterations is maximal.

The evolutionary curves of the estimated parameters are plotted in Figures 5.12,5.13,5.15,5.16. The evolutionary curves of the performance index are plotted in Figure 5.14, 5.17.

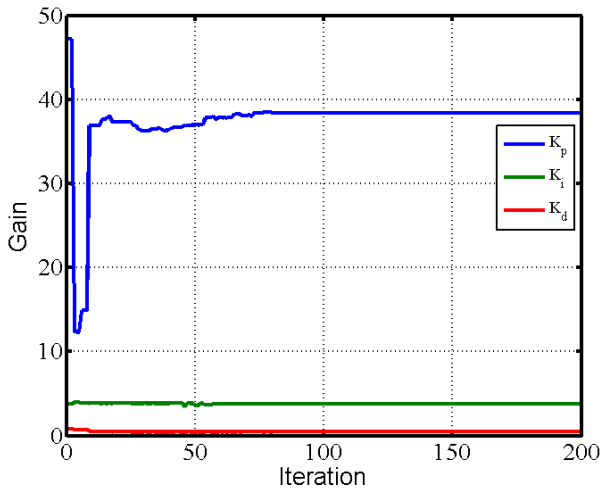

Figure 5.12: Evolutionary curve of estimated parameters (K_p, K_i, K_d) for FOPID controller with operator.

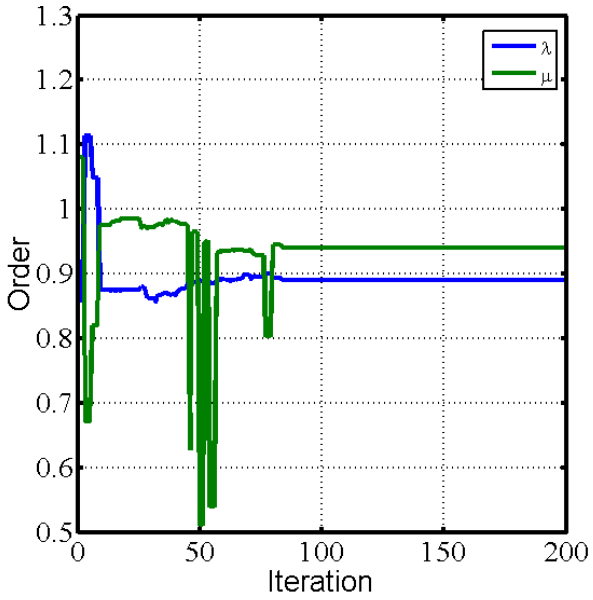

Figure 5.13: Evolutionary curve of estimated parameters (λ, μ) for FOPID controller with operator.

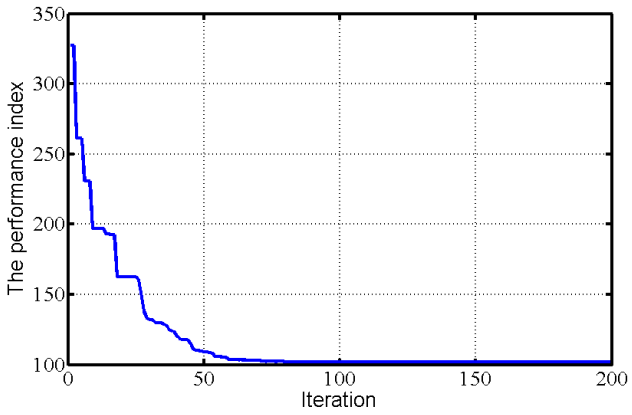

Figure 5.14: Evolutionary curve of the performance index for FOPID controller with operator.

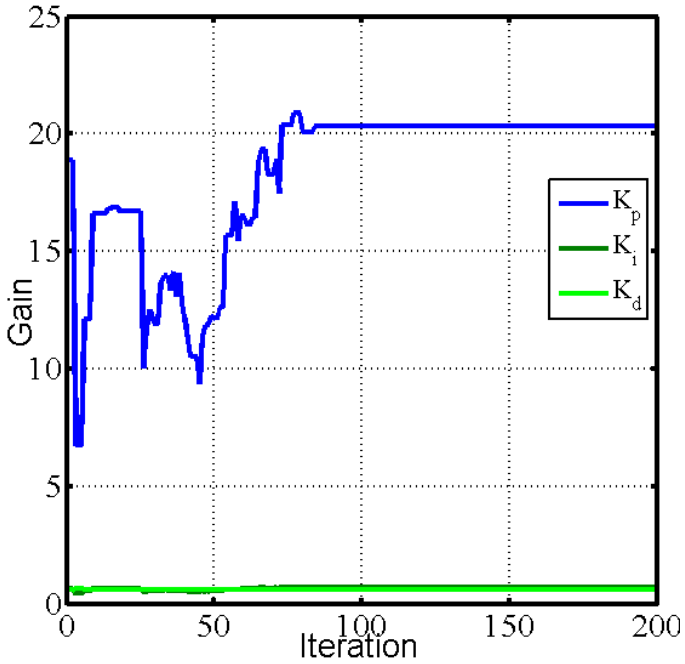

Figure 5.15: Evolutionary curve of estimated parameters (K_p, K_i, K_d) for FOPID controller without operator.

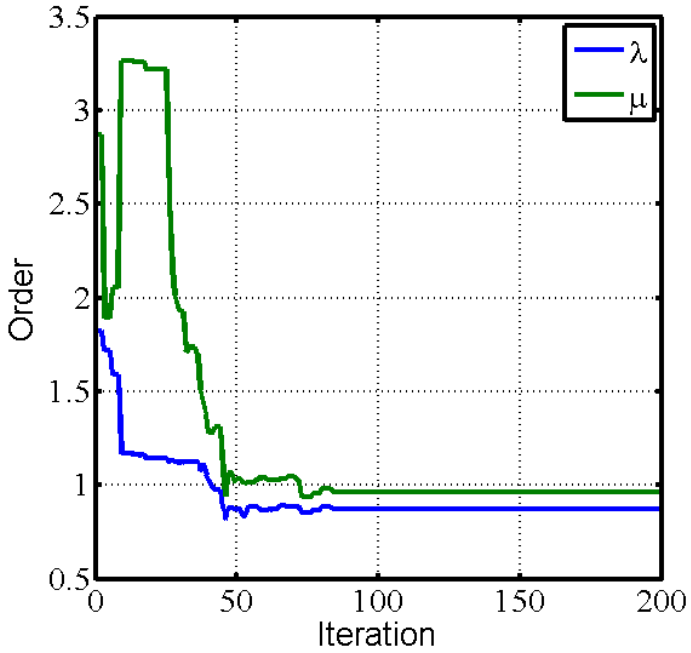

Figure 5.16: Evolutionary curve of estimated parameters (λ, μ) for FOPID controller without operator.

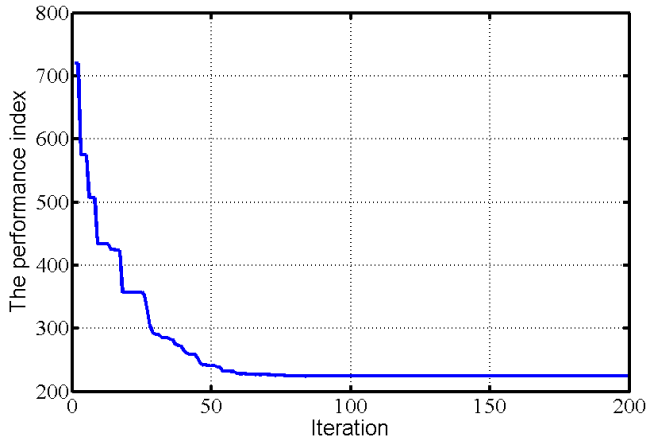

Figure 5.17: Evolutionary curve of the performance index for FOPID controller without operator.

5.6 Analysis of Performance on Tracking and Antidisturbances for the Spiral Heat Exchanger with Disturbances

In this section, the performance of the temperature control system for the spiral heat exchanger is analyzed. Two control schemes were simulated as shown in Figures 5.8 and 5.9.

5.6.1 Tracking Performance for the Spiral Heat Exchanger with Disturbances

In the simulation, a reference input signal T_r was decreased from 35 ^oC to 30 ^oC in 20 s; then, the reference input signal T_r was up to 35 ^oC. Figure 5.18 shows the operator-based fractional-order PID control scheme has better tracking performance than the fractional-order PID control scheme without operator. There is a small overshoot and a short settling time.

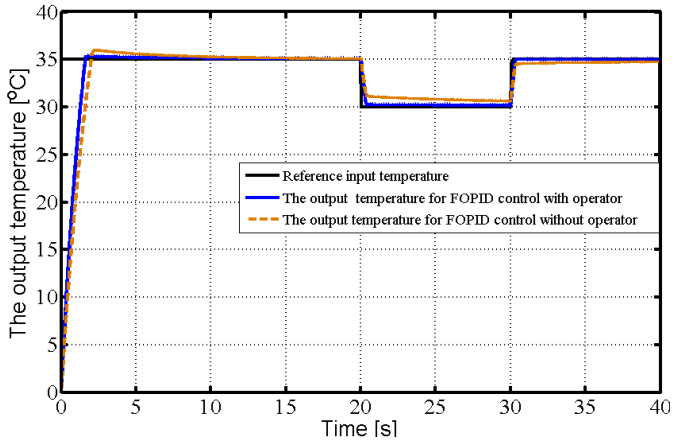

Figure 5.18: Tracking performance for the fractional-order spiral counter-flow heat exchanger.

5.6.2 Antidisturbance Performance for the Spiral Heat Exchanger

In real application, if the input flow rate of the hot-fluid side QL_1 is as control input, then the input temperature of the cold-fluid side T_{cin}, the input temperature of the hot-fluid side T_{hin}, and the input flow rate of the cold-fluid side QL_2 are three disturbances of the heat exchanger.

In the simulation, the disturbance signal T_{cin} was decreased from 20 ^oC to 15 ^oC in 20 s, T_{hin} was decreased from 50 ^oC to 45 ^oC in 20 s, and QL_1 was decreased from 5 L/Min to 3 L/Min in 20 s. Figures 5.19–5.21 show the operator-based fractional-order PID control scheme has better antidisturbance performance than the fractional-order PID control scheme without operator.

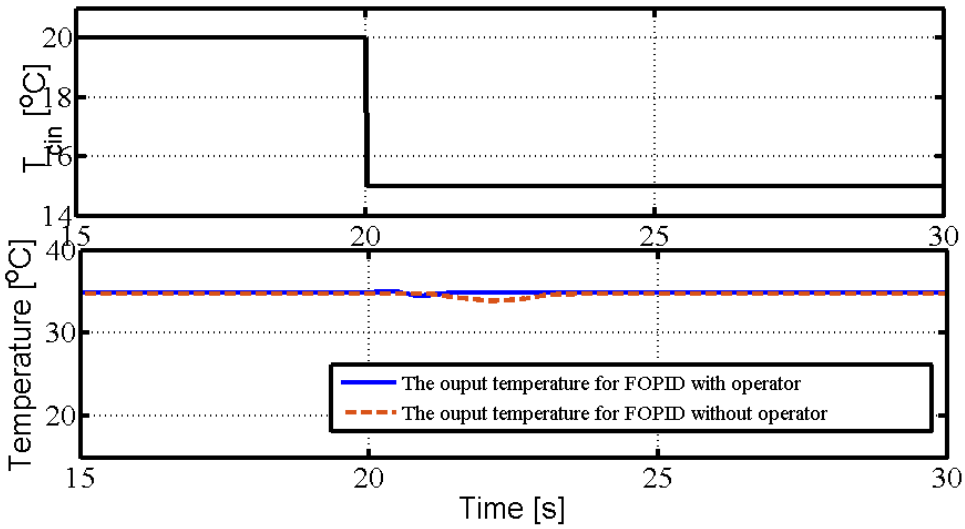

Figure 5.19: Antidisturbance performance to the input temperature of cold-fluid side.

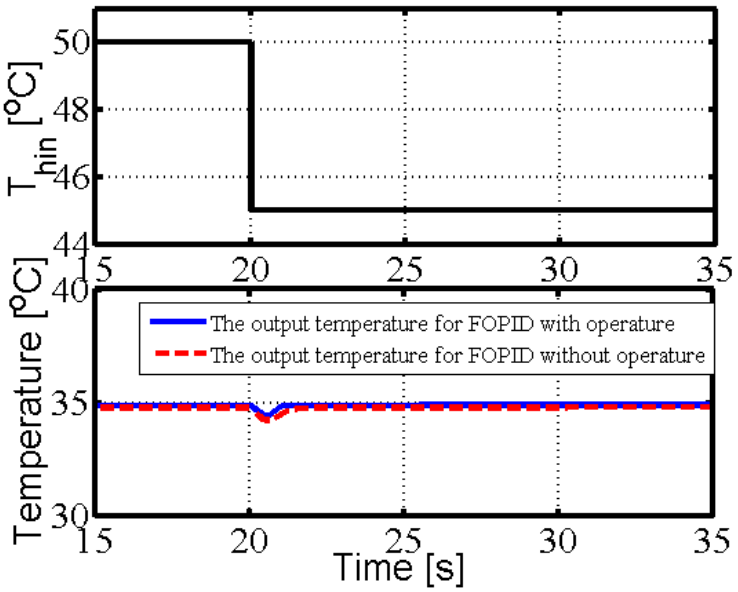

Figure 5.20: Antidisturbance performance to the input temperature of the hot-fluid side.

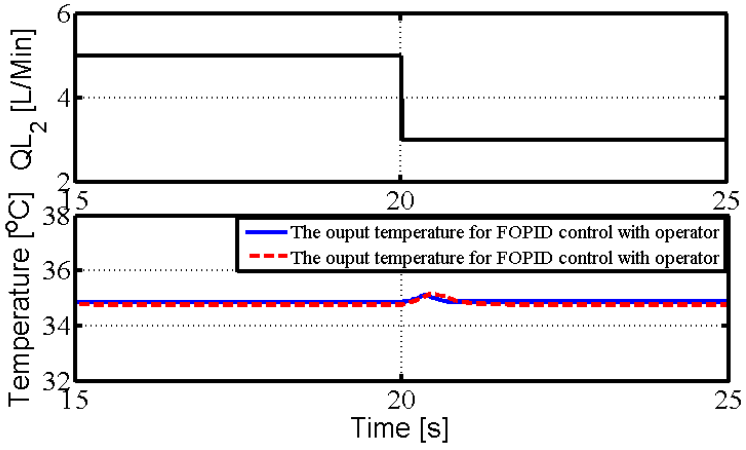

Figure 5.21: Antidisturbance performance to the input flow rate of cold-fluid side.

5.7 Conclusion

This chapter proposed operator based nonlinear fractional order robust control for the spiral counter-flow heat exchanger described by a parallel fractional-order model in order to improve the tracking performance and antidisturbance ability. The parallel fractional-order model for the spiral counter-flow heat exchanger was identified by PSO and the parameters of the fractional-order PID controller were optimized by PSO. First, the parallel fractional-order mathematical model for the spiral heat exchanger plant was identified by PSO. Second, the operator controller for the spiral heat exchanger was designed under the identified parallel fractional-order model was designed. Third, the parameters of the operator- and fractional-order-based PID controller were optimized by PSO. The tracking and antidisturbance performances of the control system were analyzed. Finally, comparisons of two control schemes were performed, and their effectiveness was illustrated.

Chapter 6

Conclusions

In this dissertation, a sapiral heat exchanger described by a parallel fractional order model with many uncertainties and disturbances is conducted. Operator & fractional order based noninear rubust contol for the spiral heat exchanger is proposed for improving control performnce.

In Chapter 2, the fractioal order preliminaries and operator theoretical background to remaining the following chapters of this dissertation is given. It also presents a spiral heat exchanger.

In Chapter 3, a parallel fractional order derivation model is proposed by considering the merit of the graphics processing unit (GPU). Then, the parallel fractional order derivation model for the spiral-plate heat exchanger is constructed. Simulations show the relationships between the output temperature of heated fluid and the orders of fractional order derivatives with two directional fluids impacted by complex factors, namely, the volume flow rate in hot fluid, and the volume flow rate in cold fluid, respectively.

Chapter 4 studies operator & fractional order based nonlinear robust control for the spiral counter-flow heat exchanger with uncertainties under disturbances. Operator fractional order controller and fractional order PID (FOPID) controller are designed and some parameters are tuned by trial-and-error method. Simulations verify tracking and anti-disturbance performance

by comparison of different control cases.

In chapter 5, operator based nonlinear fractional order robust control for the spiral heat exchanger described by a parallel fractional order model is proposed. The parallel fractional order model for the spiral heat exchanger is identified by PSO. Fractional order PID controller and operator controller for the spiral heat exchanger are design under parallel fractional order mathematical model. The parameters of FOPID controller are optimized by PSO. Finally, comparisons of two control cases are performed, and the effectiveness is illustrated.

In Chapter 6, the proposed operator & frctional order based robust nonlinear control for the spiral heat exchanger are summarized. Simulations and/or experiments have confirm their effectiveness.

Bibliography

[1] R. W. Tapre, J. P. Kaware, Review on heat transfer in spiral heat exchanger, *International Journal of Scientific Research*, vol. 5, no. 6, pp. 1–5, 2015.

[2] S. Ramachandran, P. Kalaichelvi, S. Sundaram, Heat transfer studies in a spiral plate heat exchanger for water–palm oil two phase system, *Brazilian Journal of Chemical Engineering*, vol. 25, no. 3, pp. 483–490, 2008.

[3] M. Bahiraei , A. A. Ahmadi, Thermohydraulic performance analysis of a spiral heat exchanger operated with water–alumina nanofluid: Effects of geometry and adding nanoparticles, *Energy Conversion and Management*, vol. 170, pp. 62–72, 2018.

[4] T. H. Bes, W. Roetzel, Distribution of heat flux density in spiral heat exchangers, *International Journal of Heat and Mass Transfer*, vol. 35, no. 6, pp. 1331–1347, 1992.

[5] D. K. Nguyen, J. Y. San, Effect of solid heat conduction on heat transfer performance of a spiral heat exchanger, *Applied Thermal Engineering*, vol. 76, pp. 400–409, 2015.

[6] S. Sathiyan, M Rangarajan, An experimental study of spiral-plate heat exchanger for nitrobenzene-water two-phase system, *Bulgarian Chemical Communications*, vol. 42, no. 3, pp. 205–209, 2010.

[7] J. Khorshidi, S. Heidari, Design and construction of a spiral heat exchanger, *Advances in Chemical Engineering and Science*, vol. 6, no. 2, pp. 201–298, 2016.

[8] S. Memon, P. Gadhe, S. Kulkarni, Design and testing of a spiral plate heat exchanger for textile industry, *International Journal of Scientific & Engineering Research*, vol. 10, no. 7, pp. 149–157, 2019.

[9] Y. T. Chen, S. W. Kang, W. C. Tuh, T. H. Hsiao, Experimental Investigation of Fluid Flow and Heat Transfer in Microchannels, *Tamkang Journal of Science and Engineering*, vol. 7, no. 1, pp. 11–16, 2004.

[10] V. R. Metta, R. Konijeti, A. Dasore, Thermal design of spiral plate heat exchanger through numerical modelling, *International Journal of Mechanical Engineering and Technology*, vol. 9, no. 7, pp. 736–745, 2018.

[11] P. M. Gomadam, R. E. White, J. W. Weidner, Modeling heat conduction in spiral geometries, *Journal of The Electrochemical Society*, vol. 150, no. 10, pp. A1339–A1345, 2003.

[12] M. Bidabadi, A. K. Sadaghiani, A. V. Azad, Spiral heat exchanger optimization using genetic algorithm, *Transactions on Mechanical Engineering (B)*, vol. 20, no. 5, pp. 1445–1454, 2013.

[13] S. Wen, M. Deng, Operator-based robust nonlinear control and fault detection for a Peltier actuated thermal process, *Mathematical and Computer Modelling*, vol. 57, no. 1-2, pp. 16–29, 2012

[14] R. Fujii, M. Deng, S. Wakitani, Nonlinear remote temperature control of a spiral plate heat exchanger, *Proceedings of the 2015 International Conference on Advanced Mechatronic Systems*, pp. 533–537, 2015.

[15] I. Podlubny, *Fractional Differential Equations*, Academic Press, 1999.

[16] H. Jafari, C. M. Khalique, M. Nazari, An algorithm for the numerical solution of nonlinear fractional-order Van der Pol oscillator equation, *Mathematical and Computer Modelling*, vol. 55, no. 5-6, pp. 1782–1786, 2012.

[17] R. W. Ibrahim, M. Darus, On a new solution of factional differential equation using complex transform in the unit disk, *Mathematical and Computational Applications*, vol. 19, no. 2, pp. 152–160, 2014.

[18] M. D. Ortigueira, T. H. Hsiao, A coherent approach to non-integer order derivatives, *Signal Processing*, vol. 86, no. 10, pp. 2505–2515, 2006.

[19] T. Akman Yildiz, A comparison of some control strategies for a non-integer order tuberculosis model, *An International Journal of Optimization and Control: Theories & Applications*, vol. 9, no. 3, pp. 21–30, 2019.

[20] D. Baleanu, B. Agheli, R. Darzi, An optimal method for approximating the delay differential equations of noninteger order, *Advances in Difference Equations*, https://doi.org/10.1186/s13662-018-1717-5, 2018.

[21] A. Merad, S. Hadid, Analytical solution of non-integer extra-ordinary differential equation via adomian decomposition method, *Malaya Journal of Matematik*, vol. 4, no. 1, pp. 126–135, 2016.

[22] S. Sepehr Tabatabaeia, M. Tavakoli, H. Ali Talebic, A finite-time adaptive order estimation approach for non-integer order nonlinear systems, *ISA Transactions*, https://doi.org/10.1016/j.isatra.2021.08.034, 2021.

[23] D. Qian, C. Li, R. P. Agarwal, Stability analysis of fractional differential system with Riemann–Liouville derivative, *Mathematical and Computer Modelling*, vol. 52, no. 5-6, pp. 862–874, 2010.

[24] R. Matušů, Application of fractional order calculus to control theory, *International Journal of Mathematical Models and Methods in Applied Sciences*, vol. 5, no. 7, pp. 1162–1169, 2011.

[25] S. Racewicz, F. Kutt, M. Michna, Ł. Sienkiewicz, Comparative study of integer and non-integer order models of synchronous generator, *Energies*, vol. 13, no. 17, pp. 1–11, 2020.

[26] I. Petras, *Fractional-order nonlinear systems: modeling, analysis and simulation*, Springer-Verlag, 2011.

[27] K. Kothari, U. Mehta, R. Prasad, Fractional-Order System Modeling and its Applications, *Journal of Engineering Science and Technology Review*, vol. 12, no. 6, pp. 1–10, 2019.

[28] U. D. Akpan, Stability analysis of perturbed linear non-integer differential systems, *Journal of Advances in Mathematics and Computer Science*, vol. 36, no. 6, pp. 24–29, 2021.

[29] J. Baranowski, M. Zagorowska, W. Bauer, T. Dziwinski, P. Piatek, Applications of Direct Lyapunov Method in Caputo Non-Integer Order Systems, *Elektronika ir Elektrotechnika* vol. 21, no. 2, pp. 10–13, 2015.

[30] Y. Li, Y Chen, I. Podlubny, Mittag–Leffler stability of fractional order nonlinear dynamic systems, *Automatica*, vol. 45, no. 8, pp. 1965–1969, 2009.

[31] R. Caponetto, G. Dongola, L. Fortuna, I. Petras, *Fractional Order Systems: Modeling and Control Applications*, World Scientific, 2010.

[32] S. Patnaik, S. Sidhardh, F. Semperlotti, Nonlinear thermoelastic fractional-order model of nonlocal plates: Application to postbuckling and bending response, *Thin-Walled Struct*, vol. 164, 107809, 2021.

[33] N. Challamel, D. Zorica, T. M. Atanacković, D. T. Spasić, On the fractional generalization of Eringen's nonlocal elasticity for wave propagation, *Comptes Rendus Mécanique*, vol. 341, no. 3, 298–303, 2013.

[34] R. L. Magin, M. Ovadia, Modeling the cardiac tissue electrode interface using fractional calculus, *Journal of Vibration and Control*, vol. 14, no. 9-10, pp. 1431–1442, 2008.

[35] W. Sumelka, Thermoelasticity in the Framework of the Fractional Continuum Mechanics, *Journal of Thermal Stresses*, vol. 37, no. 6, pp. 678–706, 2014.

[36] S. Sidhardh, S. Patnaik, F. Semperlotti, Thermodynamics of fractional-order nonlocal continua and its application to the thermoelastic response of beams, *European Journal of Mechanics A/Solids*, vol. 88, pp. 104238, 2021.

[37] Y. Povstenko, *Fractional Thermoelasticity*, Springer International Publishing, 2015.

[38] N. Challamel, C. Grazide, V. Picandet, A. Perrot, Y. Zhang, A nonlocal Fourier's law and its application to the heat conduction of one-

dimensional and two-dimensional thermal, *Comptes Rendus Mécanique*, vol. 344, no. 6, pp. 388–401, 2016.

[39] M. Deng, S. Wen, A. Inoue, Operator-based robust nonlinear control for a Peltier actuated process, *Measurement and Control*, vol. 44, no. 4, pp. 116–120, 2011.

[40] S. Bi, M. Deng, Y. Xiao, Robust Stability and Tracking for Operator-Based Nonlinear Uncertain Systems, *IEEE Transactions on Automation Science and Engineering*, vol. 12, no. 3, pp. 1059–1066, 2015.

[41] M. Deng, T. Kawashima, Adaptive Nonlinear Sensorless Control for an Uncertain Miniature Pneumatic Curling Rubber Actuator Using Passivity and Robust Right Coprime Factorization, *IEEE Transactions on Control Systems Technology*, vol. 24, no. 1, pp. 318–324, 2016.

[42] G. Dong, M. Deng, Modeling of a spiral heat exchanger using fractional order equation and GPU, *Proceedings of the 2019 International Conference on Advanced Mechatronic Systems (ICAMechS)*, pp. 108–113, 2019.

[43] A. Magadum, A. Pawar, R. Patil, R. Phadtare, T. C. Mestri, Review of experimental analysis of parallel and counter flow heat exchanger, *International Journal of Engineering Research & Technology (IJERT)*, vol. 5, no. 2, pp. 395–397, 2016.

[44] T. Bergman, A. Lavine, F. Incropera, D. Dewitt, *Faundamentals of Heat and Mass Transfer*, 2017.

[45] G. Dong, M. Deng, M. GPU Based Modelling and Analysis for Parallel Fractional Order Derivative Model of the Spiral-Plate Heat Exchanger, *Axioms*, vol. 344, pp. 1–25, 2021.

[46] G. Dong, M. Deng, Operator Based Fractional Order Control System for a Spiral Heat Exchanger with Uncertainties, *Proceedings of the 2021 International Conference on Advanced Mechatronic Systems (ICAMechS)*, pp. 242–247, 2021.

[47] A. Sandhya, R. Sandhya, M. Prameela, An overview of Fractional order PID Controllers and its Industrial applications, *International Journal of Innovations in Engineering and Technology*, vol. 6, no. 4, pp. 534–546, 2016.

[48] V. Shekher, P. Rai, O. Prakash, Tuning and Analysis of Fractional Order PID Controller, *International Journal of Electronic and Electrical Engineering*, vol. 5, no. 1, pp. 11–21,2012.

[49] S. Swati, H. Yogesh, Fractional Order Controller and its Applications: A Review, *Proceedings of the IASTED Asian Conference*, pp. 1–6, 2012.

[50] R. Ranganayakulu, G. Uday Bhaskar Babu, A. Seshagiri Rao, D. Shikchand Patle, A comparative study of fractional order PI^{λ} / $PI^{\lambda}D^{\mu}$ tuning rules for stablefirst order plus time delay processes, *Resource-Efficient Technologies*, vol. 2, pp. S136–S152, 2016.

[51] T. Doğruer, A. Yüce, N. Tan, PID controller design for a fractional order system using bode's ideal transfer function, *International Journal of Engineering Research and Development*, vol. 9, no. 3, pp. 126–135, 2017.

[52] M. Dulăua, A.Gligor, T. M. Dulău, Fractional Order Controllers Versus Integer Order Controllers, *Procedia Engineering*, vol. 181, pp. 538–545, 2017.

[53] L. Chen, N. Saikumar, S. H. HosseinNia, Development of robust fractional-order reset control, *IEEE Transactions on Control Systems Technology*, vol. 28, no. 4, pp. 1404–1417, 2020.

[54] A. G. S. Sánchez, J. Soto-Vega, E. Tlelo-Cuautle, M. A. Rodríguez-Licea, Fractional-order approximation of PID controller for buck–boost converters, *Micromachines*, vol. 12, no. 6, pp. 1–16, 2021.

[55] P. Mercader, A. BañosA, PI tuning rule for integrating plus dead time processes with parametric uncertainty, *ISA Transactions*, vol. 67, pp. 246–255, 2017.

[56] K. Ghousiya Begum, A. Seshagiri Rao, T.K. Radhakrishnan, Enhanced IMC based PID controller design for non-minimum phase (NMP) integrating processes with time delays, *ISA Transactions*, vol. 68, pp. 223–234, 2017.

[57] B. Yang, T. Yub, H. Shua, D. Zhua, N. An, Y. Sang, L. Jiang, Energy reshaping based passive fractional-order PID control design and implementation of a grid-connected PV inverter for MPPT using grouped grey wolf optimizer, *Solar Energy*, vol. 170, pp. 31–46, 2018.

[58] S. Das, I. Pan, S. Das, A. Gupta, Improved model reduction and tuning of fractional-order PIλDμ controllers for analytical rule extraction with genetic programming, *ISA Transactions*, vol. 51, pp. 237–261, 2012.

[59] A. Ateş, C. Yeroglu, Optimal fractional order PID design via Tabu Search based algorithm, *ISA Transactions*, vol. 60, pp. 109–118, 2016.

[60] H. Sabina Sanchez, F. Padula , A. Visioli , R. Vilanova, Tuning rules for robust FOPID controllers based on multi-objective optimization with FOPDT models, *ISA Transactions*, vol. 66, pp. 344–361, 2017.

[61] C. A. Monje, Y. Chen, B. M. Vinagre, D. Xue, V. Feliu, *Fractional Order Systems and Controls: Fundamentals and Applications*, Springer, 2010.

[62] K. B. Oldham, J. Spanier, *The Fractional Calculus: Theory and Applications of Differentiation and Integration to Arbitrary Order*, Dover Publications, 2006.

[63] J. Padovan, Computational algorithms for FE formulations involving fractional operator, *Computational Mechanics*, vol. 2, pp. 271–287, 1987.

[64] L. Zhong, Comparative analysis of GPU and CPU, *Journal of Open Innovation: Technology, Market, and Complexity*, vol. 9, pp. 13–14, 2009.

[65] E. Buber, B. Diri, Analysis and CPU vs GPU Comparison for Deep Learning, *2018 6th International Conference on Control Engineering & Information Technology (CEIT)*, 2018, pp. 1-6, doi: 10.1109/CEIT.2018.8751930.

[66] S. Liu, M Liu, G. Zhang, Model of accelerating MATLAB computation based on CUDA, *Applied Research Compute*, vol. 6, pp. 2140–2143, 2010.

[67] M. Deng, A. Inoue, Q. Zhu, An integrated study procedure on real time estimation of time varying multijoint human arm viscoelasticity, *Transactions of the Institute of Measurement and Control*, vol. 33, no. 8, pp. 919–941, 2011.

[68] R. Caponetto, G. Dongola, L. Fortuna, I. Petras, *Fractional Order Systems: Modeling and Control Applications*, World Scientific, 2010.

[69] R. Fujii, M. Deng, S. Wakitani, Nonlinear remote temperature control of a spiral plate heat exchanger, *Proceedings of the 2015 International Conference on Advanced Mechatronic Systems*, pp. 533–537, Beijing, China, 2015.

[70] S. Wen, M. Deng, A. Inoue, Operator-based robust nonlinear control for gantry crane system with soft measurement of swing angle, *International*

Journal of Modelling, Identification and Control, vol. 16 no. 1, pp. 86–96, 2012.

[71] A. Wang, M. Deng, Robust nonlinear multivariable tracking control design to a manipulator with unknown uncertainties using operator-based robust right coprime factorization, *Transactions of the Institute of Measurement and Control*, vol. 35, no. 6, pp. 788–797, 2013.

[72] M. Deng, *Operator-Based Nonlinear Control Systems: Design and Applications*, Wiley-IEEE Press, 2014.

[73] L. Jiang, M. Deng and A. Inoue, A SVM-based two wheeled mobile robot motion control in stochastic environments, *Proceedings of the Institution of Mechanical Engineers, Part I: Journal of Systems and Control Engineering*, vol. 222, no. 7, pp. 733-743, 2008.

[74] L. Jiang, M. Deng and A. Inoue, Obstacle avoidance and motion control of a two wheeled mobile robot using SVR technique, *International Journal of Innovative Computing Information and Control*, vol. 5, no. 2, pp. 253-262, 2009.

[75] T. Nguyen Luan Vu, M. Lee, Analytical design of fractional-order proportional-integral controllers for time-delay processes, *ISA Transactions*, vol. 52, pp. 583–591, 2013.

[76] J. C. Travieso-Torres, M. A. Duarte-Mermoud, O. Beytia, Combining fractional order operators and adaptive passivity-based controllers: an application to the level regulation of a conical tank, *CONTROL ENGINEERING AND APPLIED INFORMATICS*, vol. 19, no. 2, pp. 3–10, 2017.

[77] A. Biswas, S. Das, A. Abraham, S. Dasgupta, Design of fractional-order $PI^{\lambda}D^{\mu}$ controllers with an improved differential evolution, *Engineering Applications of Artificial Intelligence*, vol. 22, no. 2, pp. 343–350, 2009.

[78] A. Djari, T. Bouden, A. Boulkroune, Design of fractional-order PID controller (FOPID) for a class of fractional-Order MIMO Systems using a particle swarm optimization (PSO) approach, *Proceedings of the 3rd International Conference on Systems and Control*, pp. 1–6, Algiers, Algeria, 2013.

[79] N. Aguila-Camacho, M. A. Duarte-Mermoud, Fractional adaptive control for an automatic voltage regulator, *ISA Transactions*, vol. 52, no. 6, pp. 807–815, 2013.

[80] R. El-Khazali, Fractional-order $PI^{\lambda}D^{\mu}$controller design, *Computers & Mathematics with Applications*, vol. 66, no. 5, pp. 639–646, 2013.

[81] S. Ijaz, M. T. Hamayun, L. Yan, and M. F. Mumtaz, Fractional order modeling and control of twin rotor aero dynamical system using nelder mead optimization, *Journal of Electrical Engineering and Technology*, vol. 11, no. 6, pp. 1863–1871, 2016.

[82] M. Bettayeb, R. Mansouri, Fractional IMC-PID-filter controllers design for non integer order systems, *Journal of Process Control*, vol. 24, no. 4, pp. 261–271, 2014.

[83] F. A. Hasan, L. J. Rashad, Fractional-order PID controller for permanent magnet DC motor based on PSO algorithm, *International Journal of Power Electronics and Drive System*, vol. 10, no. 4, pp. 1724–1733, 2019.

[84] C. Yin, Y. Q. Chen, S. Zhong, Robust stability and stabilization of uncertain fractional-order descriptor nonlinear system, *Proceedings of the*

19th World Congress The International Federation of Automatic Control, pp. 6080–6085, Cape Town, South Africa, 2014.

[85] F. Isdaryani, F. Feriyonika, R. Ferdiansyah, Comparison of Ziegler-Nichols and Cohen Coon tuning method for magnetic levitation control system, *International Conference on Applied Science and Technology (iCAST on Engineering Science)*, pp. 1–10, Bali, Indonesia, 2019.

[86] L. Liu, S. Zhang, Robust fractional-order PID controller tuning based on bode's optimal loop shaping, *Complexity*, https://doi.org/10.1155/2018/6570560, 2018.

[87] F. Padula, A. Visioli, Tuning rules for optimal PID and fractional-order PID controllers, *Journal of Process Control*, vol. 21, no. 1, pp. 69–81, 2011.

[88] D. Valério, J. da Costa, Ziegler-Nichols type tuning rules for fractional PID controllers, pp. 1431-1440, https://doi.org/10.1115/DETC2005-84344, 2008.

[89] J. Kennedy, R. Eberhart, Particle Swarm Optimization. *Proceedings of the ICNN'95—International Conference on Neural Networks*, pp. 1942–1948, 1995.

[90] D. Pal, P. Verma, D. Gautam, P. Indait, Improved optimization technique using hybrid ACO-PSO. *Proceedings of the 2016 2nd International Conference on Next Generation Computing Technologies*, pp. 277–282, 2016.

[91] T. Hendtlass, WoSP: A multi-optima particle swarm algorithm. *Proceedings of the IEEE Congress on Evolutionary Computation*, pp. 727–734,2005.

Appendix A

A spiral heat exchanger plant

A.1 A Spiral Heat Exchanger Plant

A spiral heat exchanger is shown in Figure A.1. This design has many merits, such as a highly efficient heat transfer, small size in comparison to other heat exchangers, and self-cleaning capability thanks to the unique spiral structure.

Figure A.1: A spiral heat exchanger plant.

The spiral heat exchanger is an piece of excellent heat transfer equipment; however, its complex inner structure makes it difficult to built an accurate

mathematical model. Generally, the logarithmic mean temperature difference method is used, however, control performance is bad. We considered using a fractional order derivative equation to describe a spiral heat exchanger. Figure A.2 shows a cross-section of the inner structure of the spiral-plate heat exchanger, where δ_h , δ_c, and δ_s represent the width of hot fluid, the width of cold fluid and the width of solid wall, respectively. In this paper, the inner cold fluid, as shown in Figure A.2, is divided into a micro-volume. A fractional order derivative equation is constructed by considering the heat balance of the two fluids.

$$r = b + a \cdot \theta, \theta \in [0, 11\pi] \tag{A.1}$$

The geometric parameters of the spiral-plate heat exchanger are denoted in Table A.1.

Table A.1: Parameters of the spiral-plate heat exchanger.

Meaning	**Symbol**	**Value**
Geometric parameter of a spiral function	a	$\frac{0.005}{\pi}$ m/rad
Initial radius of hot fluid side	b	0.08 m
Spiral function angle of the spiral-plate heat exchanger	θ	$[0, 11\pi]$
The width of hot flow channel	δ_h	0.005 m
The width of cold flow channel	δ_c	0.005 m
The width of solid wall	δ_s	0.0018 m
The height of the spiral-plate heat exchanger	Z	0.011 m

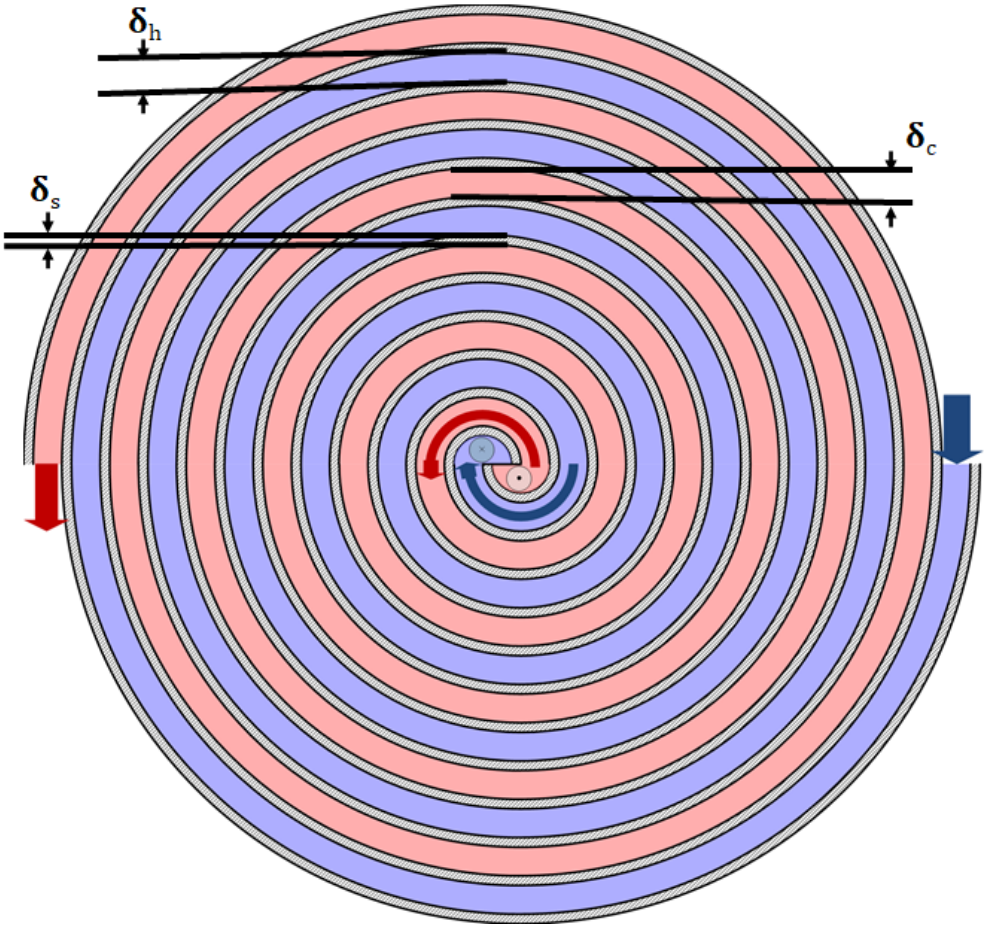

Figure A.2: Cross-section of the inner structure of the spiral-plate heat exchanger.

Heat exchangers are typically classified into parallel-flow and count-flow types based on their arrangement. In the parallel-flow type, both the input and the output of the two directional fluids (one a hot fluid, the other a cold fluid) flow in the same direction. In a counter-flow heat exchanger, the hot fluid and cold fluid flow in opposite directions. In this paper, we study a fractional order derivative model of a spiral counter-flow type heat exchanger.

Publications

Journal papers

1. **G. Dong** and M. Deng, GPU Based Modelling and Analysis for Parallel Fractional Order Derivative Model of the Spiral-Plate Heat Exchanger, *Axioms*, vol. 10, no. 4: 344, pp. 1-25, 2021. (Chapter 3; Web of Science (IF 1.824));

2. **G. Dong** and M. Deng, Operator & Fractional Order Based Nonlinear Robust Control for a Spiral Counter-flow Heat Exchanger with Uncertainties and Disturbances, *Machines*, vol. 10, no. 5: 335, pp. 1-18, 2022. (Chapter 4; Web of Science (IF 2.899))

3. **G. Dong** and M. Deng, Operator-Based Fractional-Order Nonlinear Robust Control for the Spiral Heat Exchanger Identified by Particle Swarm Optimization, *Electronics*, vol. 11, no. 17: 2800, pp. 1-20, 2022. (Chapter 5; Web of Science (IF 2.690))

Proceedings papers

1. **G. Dong**, M. Deng, L. Jin, Modeling of a spiral heat exchanger using fractional order equation and GPU, *Proceedings of the 2019 International Conference on Advanced Mechatronic Systems*, pp. 108-113, August 26-28, 2019, Kusatsu, Shiga, Japan. (Chapter 3, 5; Web of Science)

2. **G. Dong**, M. Deng, Operator Based Fractional Order Control System for a Spiral Heat Exchanger with Uncertainties, *Proceedings of the 2021 International Conference on Advanced Mechatronic Systems*, pp. 242-247, December 9-12, 2021, Tokyo, Japan. (Chapter 4, 5; Web of Science)

Other papers

1. **G. Dong**, M. Deng, Modelling of parallel fractional order model for the spiral-plate heat exchanger, *Proceedings of the 2022 IEEJ Annual Conference on Control*, pp. 1-4, January 7-9, 2022, Tokyo, Japan.